Analyses of Scatterometer and SAR Data at the University of Hamburg

Wind, Waves, Surface Films and Rain

ГАДЕ, Мартин Хорстович (aka Martin Gade)
Institut für Meereskunde, Universität Hamburg, Германия

Outline

- SAR Examples
- Surface Films: Scat and SAR
- Rain on Scat and SAR data
- Multi³ Scat Experiments
- Wind Scat and Ocean Color
- Summary

Synthetic Aperture Radar (SAR)

SAR sensors aboard satellites

ERS-1/2 (1991 / 1995)

ENVISAT (2002)

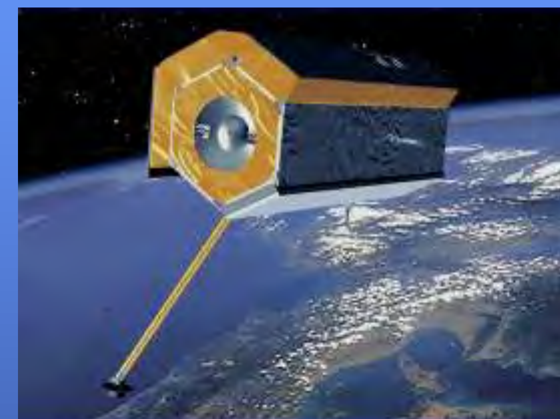

TerraSAR-X (2007)

RADARSAT-1/2 (1995 / 2007)

ALOS (2006)

further SARs on Indian, Chinese, Russian satellites

SAR Examples (1)

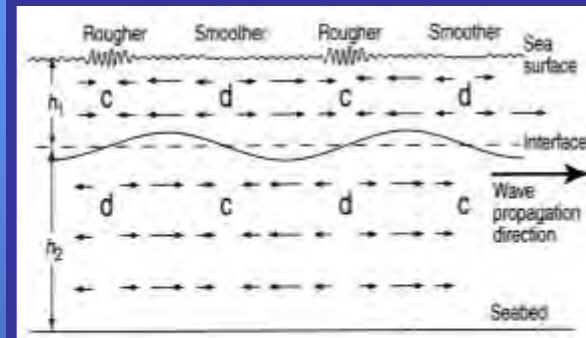

[Robinson, 2003]

ERS SAR image (100 km × 100 km)
Strait of Gibraltar
(1 January 1993, 2239 UTC, © ESA)

SAR Examples (2)

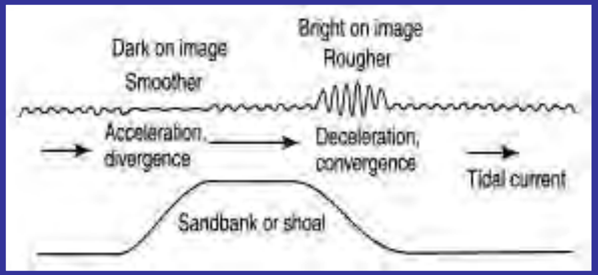

[Robinson, 2003]

ERS SAR image (100 km × 100 km)
Chinese coast
(8 July 1995, 0234 UTC, © ESA)

SAR Examples (3)

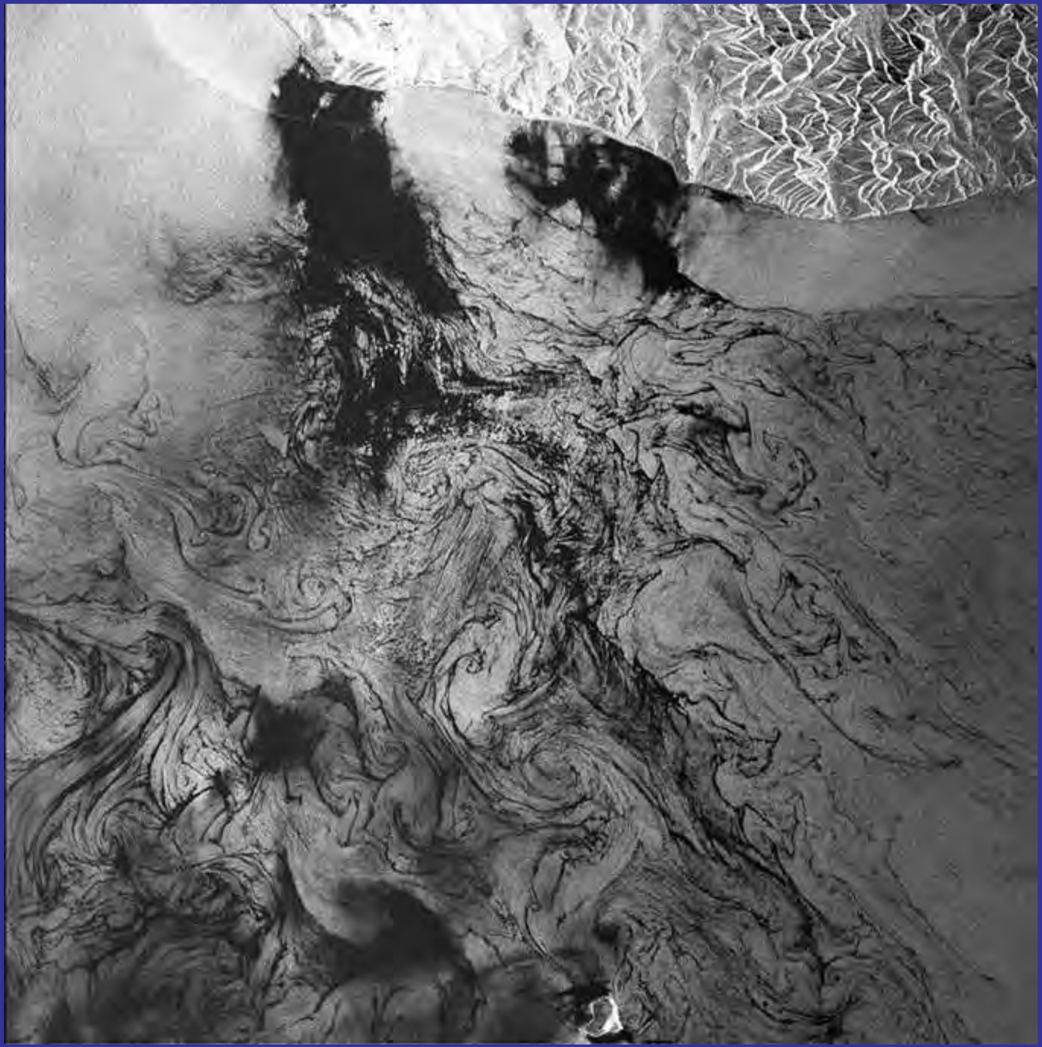

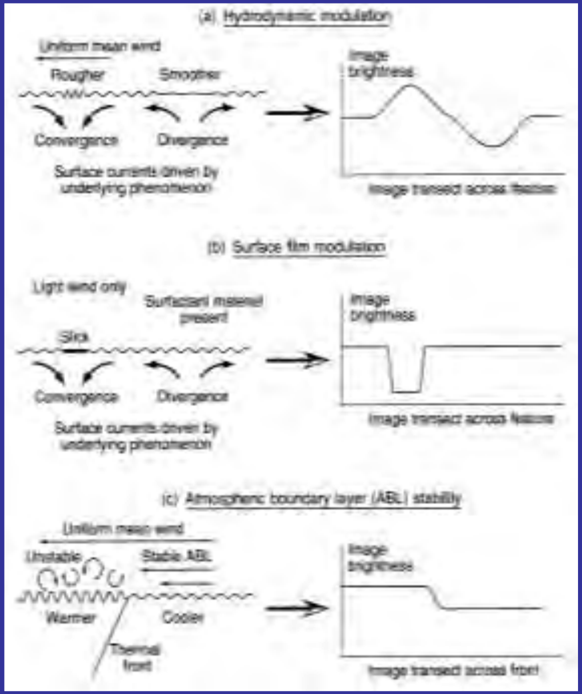

[Robinson, 2003]

ERS SAR image (70 km × 70 km)
Bering Strait
(24 June 1997, © ESA)

SAR Examples (4)

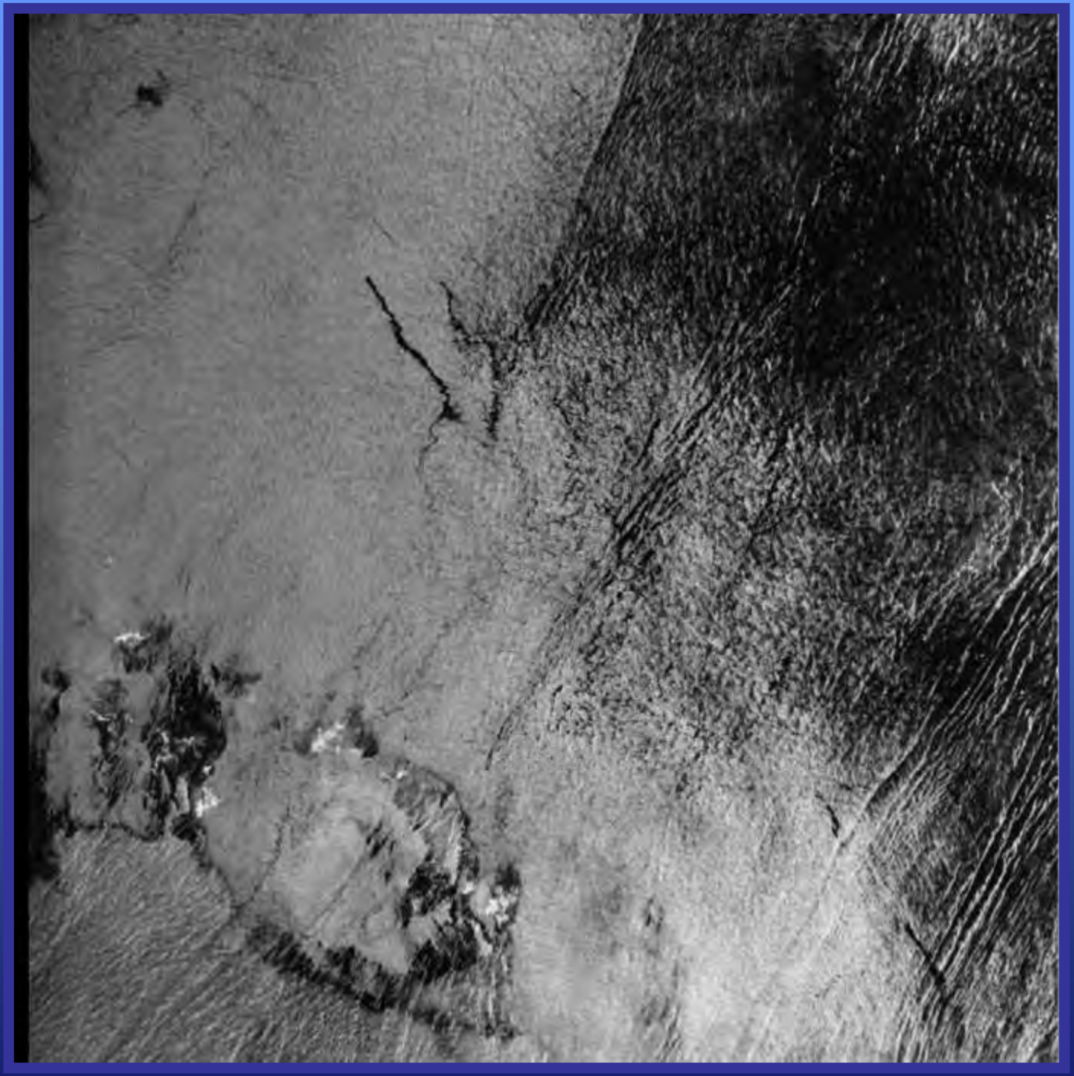

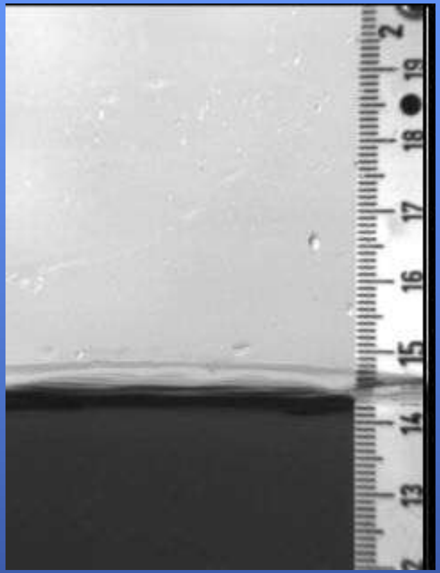

ERS SAR image (100 km × 100 km)
South China Sea
(14 May 1998, 0252 UTC, © ESA)

SAR Examples (5)

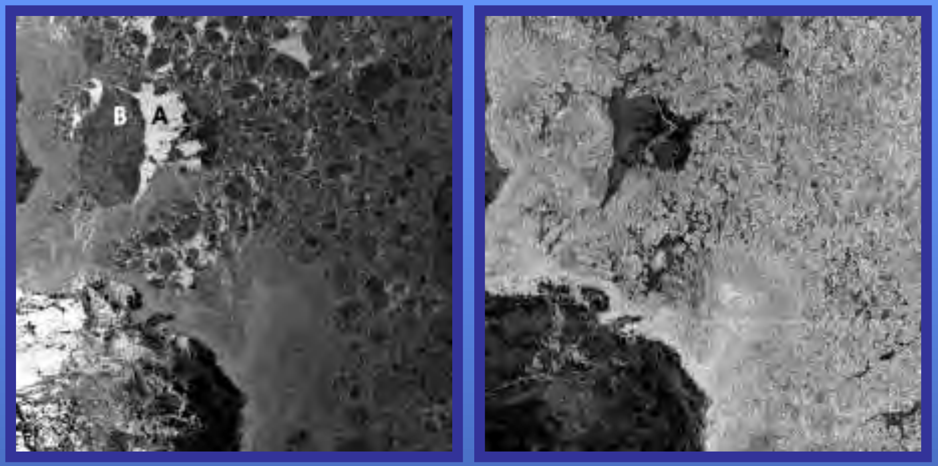

[Barale & Gade 2008]

SAR images (80 km × 80 km)
Arctic sea ice at 82°N 12°E
(19 September 1996, © ESA, CSA)
left: ERS (C Band, VV pol)
right: Radarsat (C Band, HH pol)

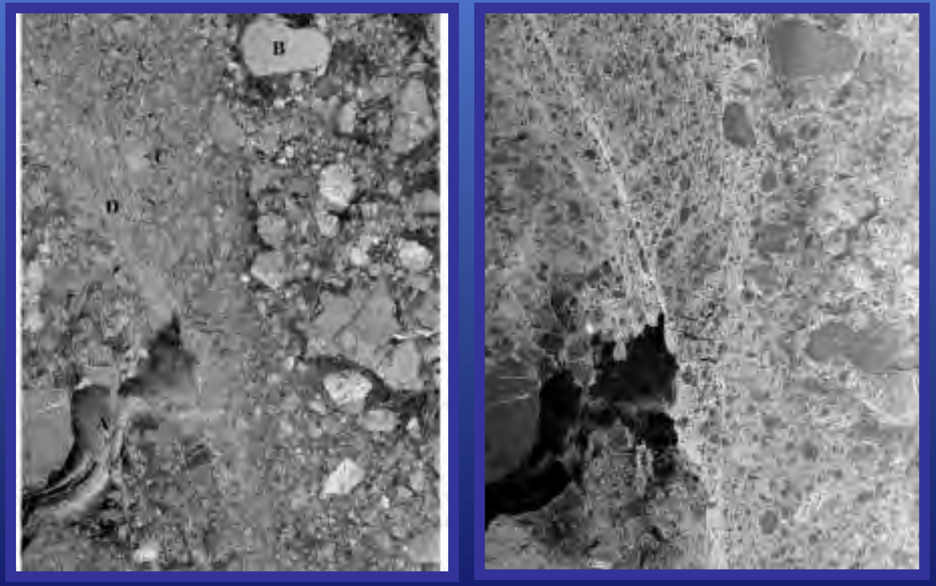

ERS SAR image (50 km × 65 km)
Arctic sea ice
(© ESA, NASDA)
left: ERS (C Band, VV pol)
right: JERS-1 (L Band, HH pol)

Surface Films

Surface Films on SAR Images

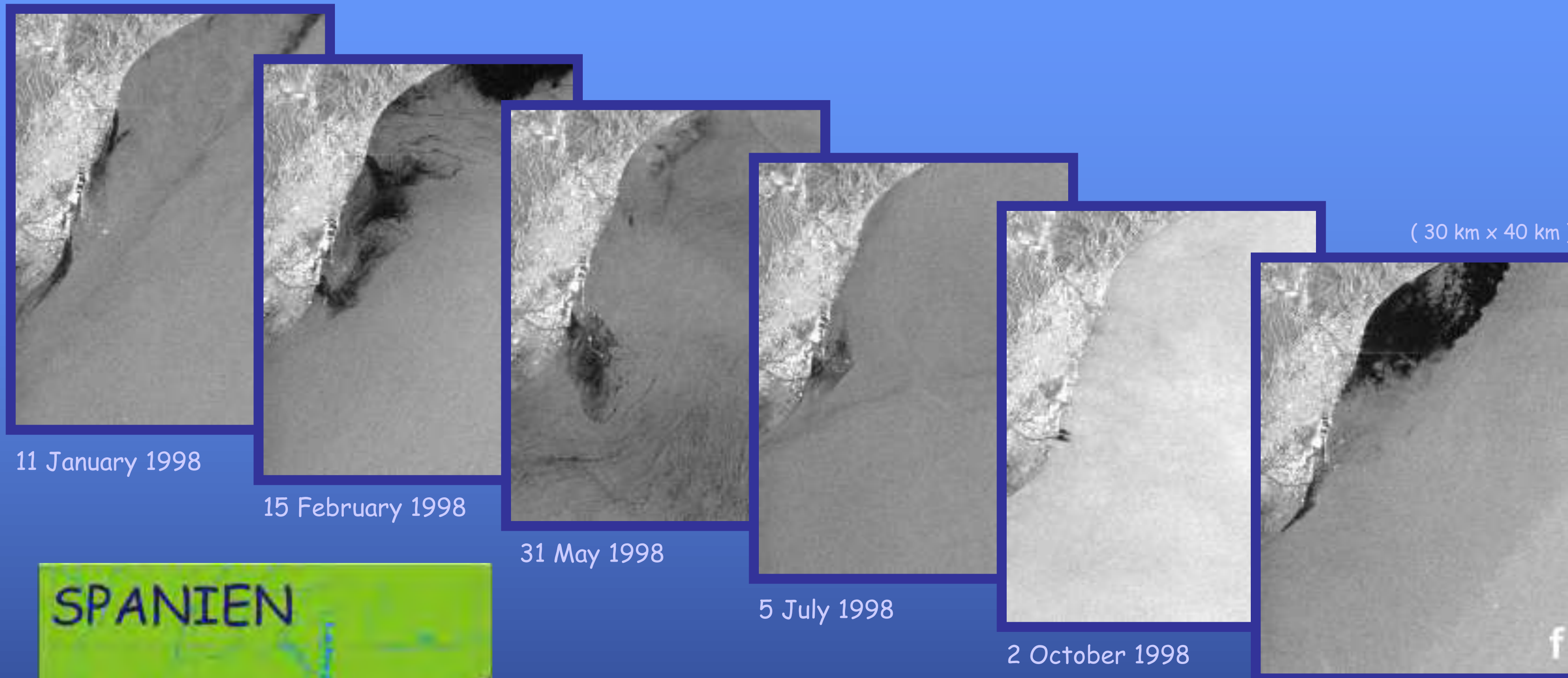

ERS SAR images (30 km × 40 km)
of the north-western Med, off Barcelona
(© ESA)

Anthropogenic Surface Films on SAR Images

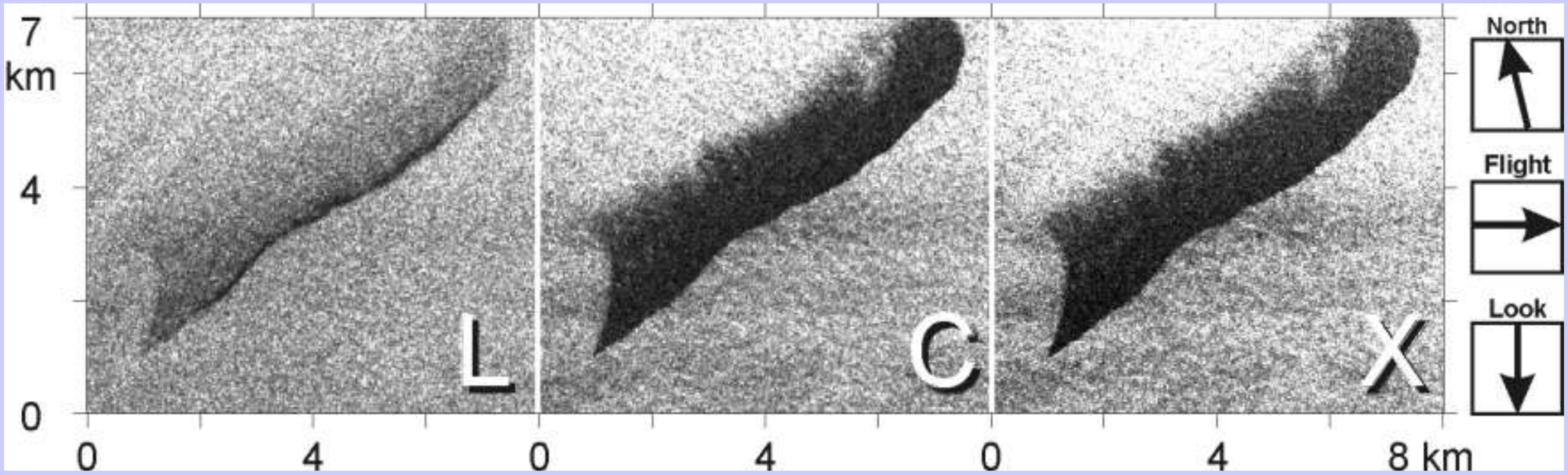

damping ratios of various mineral oil spills:

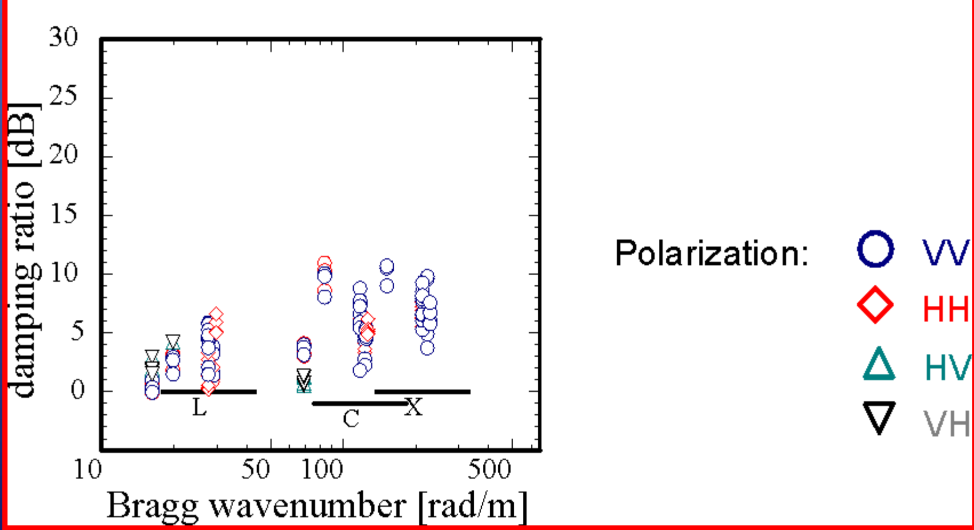

SIR-C/X-SAR

Baltic Sea

e.g., 9 April 1994

Monotonous increase of damping ratios

No dependency on polarization

Biogenic Surface Films on SAR Images

High damping ratios at low wavenumbers

No dependency on polarization

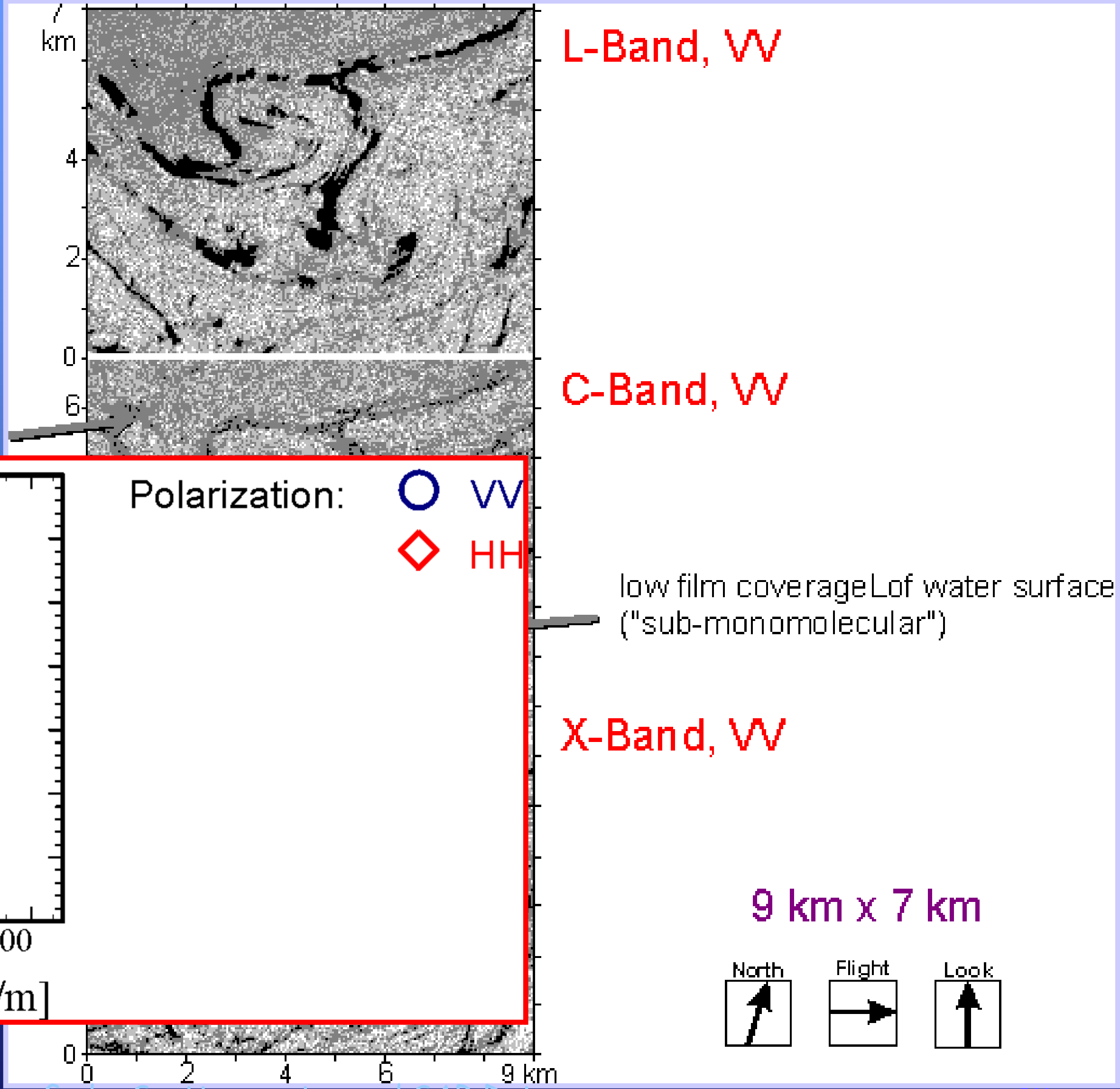

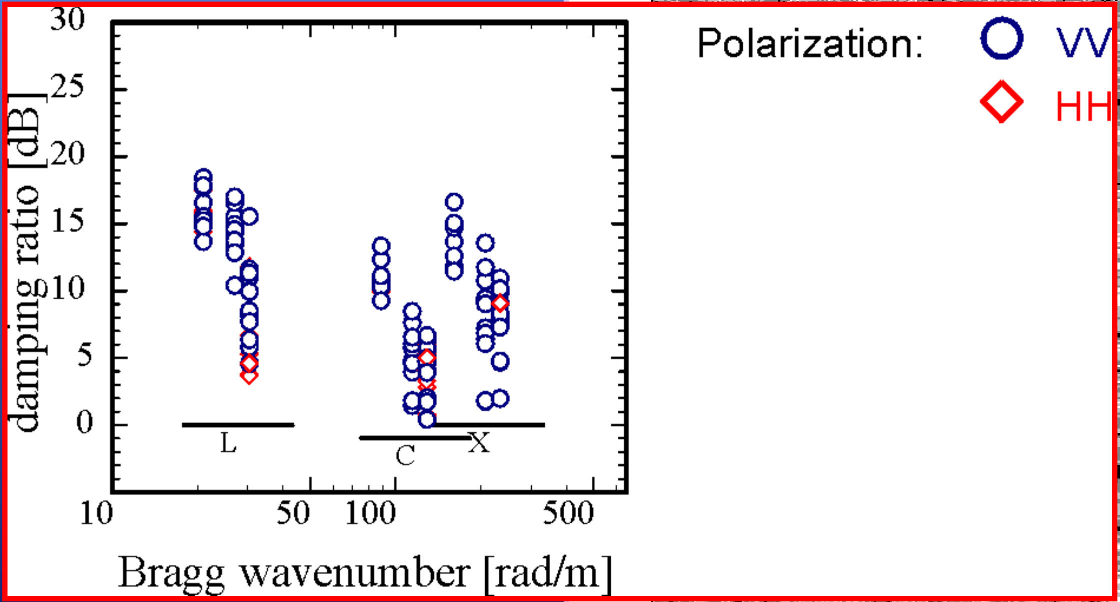

Wave Damping by Surface Films

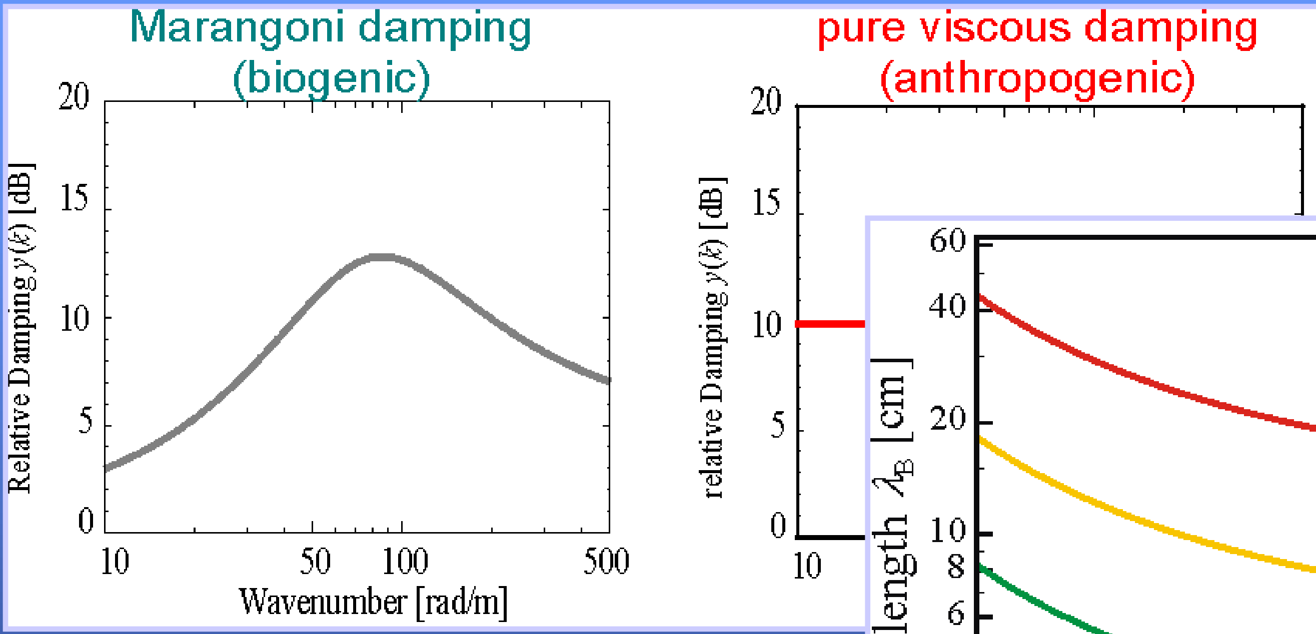

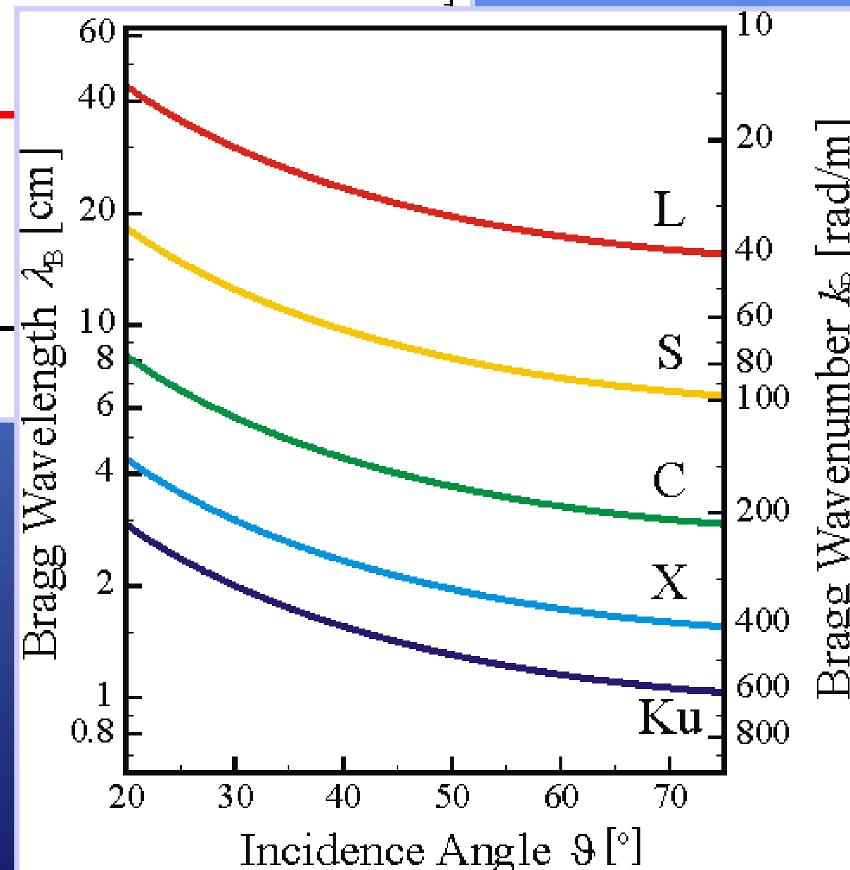

Use multi-frequency radar techniques to discriminate between biogenic and anthropogenic surface films

Field Experiments With Artificial Surface Films

<u>Multi³ SCAT of Univ Hamburg:</u>

- Flown on helicopter BO 105
- 5 frequencies: (L, S, C, X, Ku band)
- 4 polarisations (HH, HV, VV, VH)
- Incidence angle: 23° ... 65°
- nomin. flight altitude: 150 m
- Ø footprint: 1.6 m ... 128.9 m
- Transmit power: 10 mW ... 150 mW

Field Experiments With Artificial Surface Films

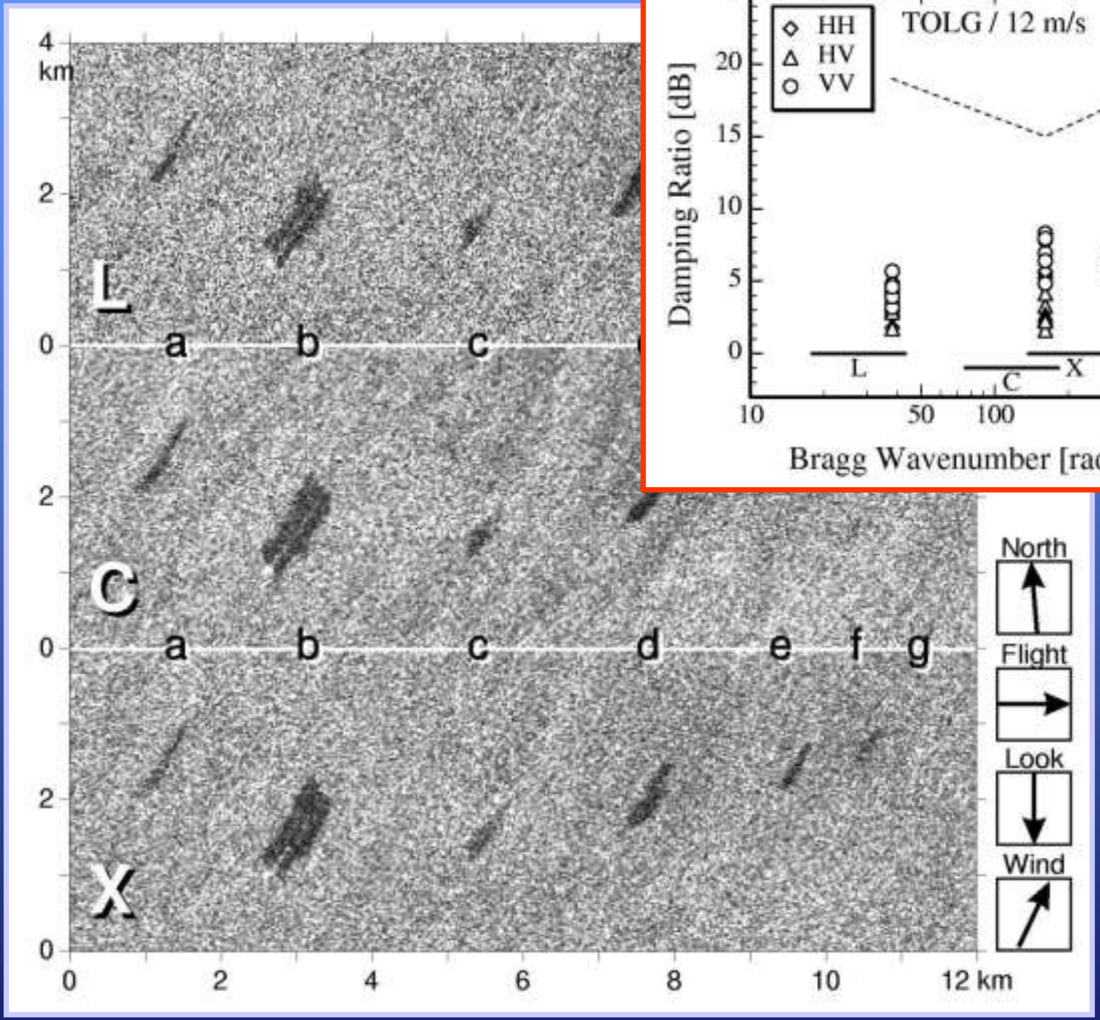

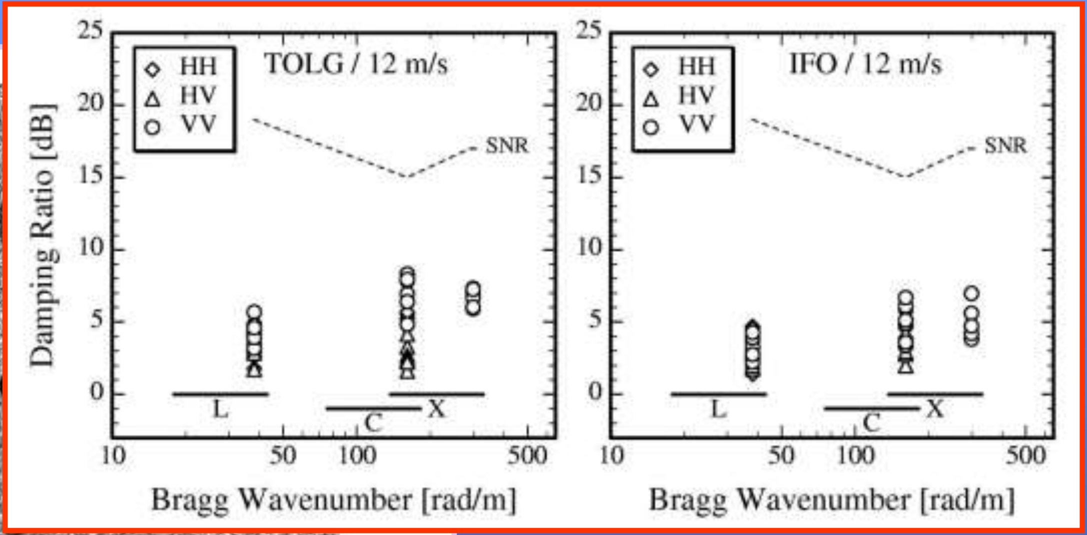

1994: 2 SIR-C/X-SAR missions

Field experiments with quasi-biogenic slicks and anthropogenic oil spills

Just minor differences in radar contrast at high wind speeds (12 m/s)

Field Experiments With Artificial Surface Films

5-frequency/multi-polarization HELISCAT

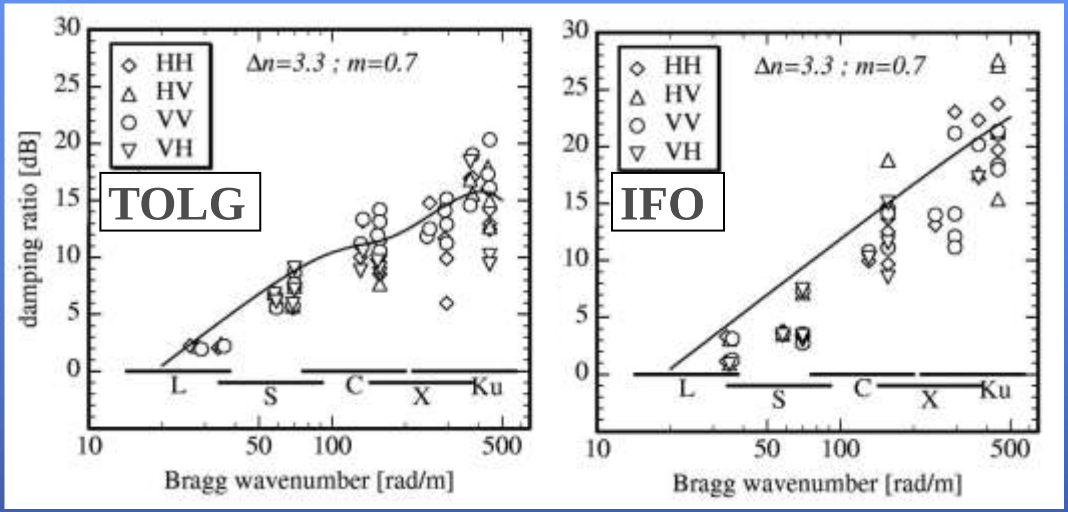

Modeling damping ratios at high wind speeds

$$\frac{\sigma^{(0)}(k)}{\sigma^{(s)}(k)} = \frac{\Psi_0(k)}{\Psi_s(k)} \approx \frac{\beta_s - 2\Delta_s c_g}{\beta_0 - 2\Delta_0 c_g} \cdot m^{\Delta n - 4} \left(2u_* \cdot \sqrt{\frac{|\cos\varphi| k}{g}} \right)^{\Delta n}$$

m : parameter describing reduction of friction velocity
Δn : parameter describing reduction of wave breaking

Model can explain

monotonous increase of damping curves (no Marangoni maximum!)

similar damping behavior of biogenic and anthropogenic films

Field Experiments With Artificial Surface Films

Comparison of SIR-C/X-SAR and HELISCAT results

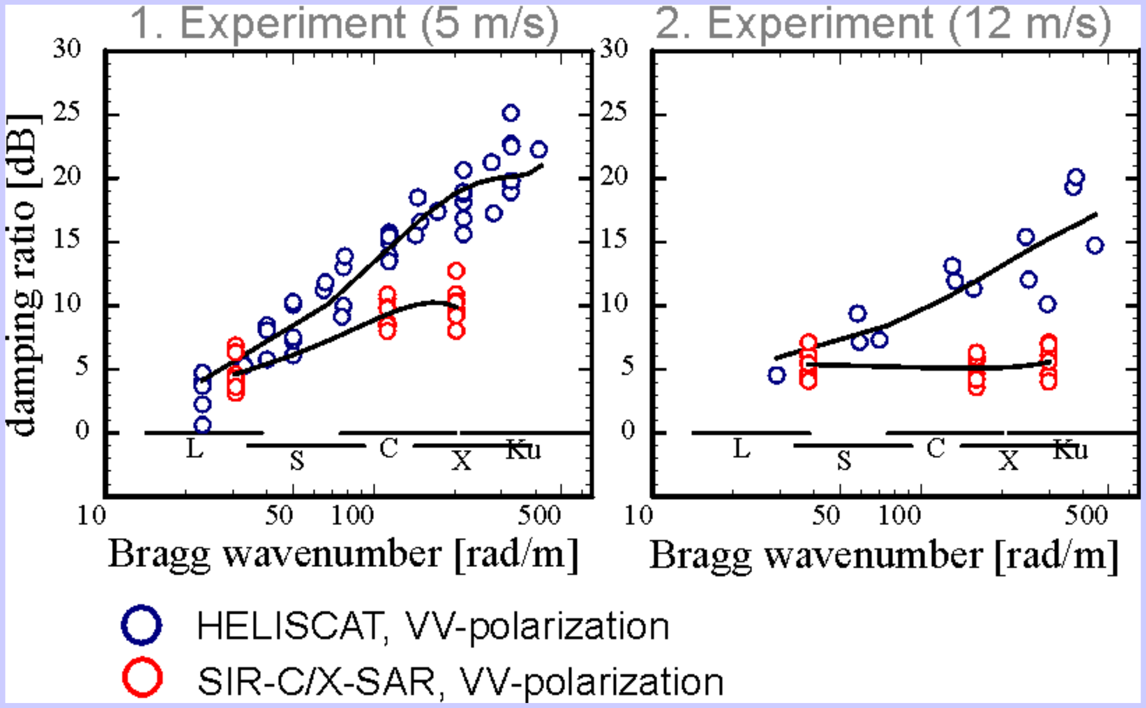

HELISCAT measured higher damping ratios !

Difference depends on type of sensor ?

Statistical Analysis of SAR Images

Oil Pollution Observed in European Marginal Seas

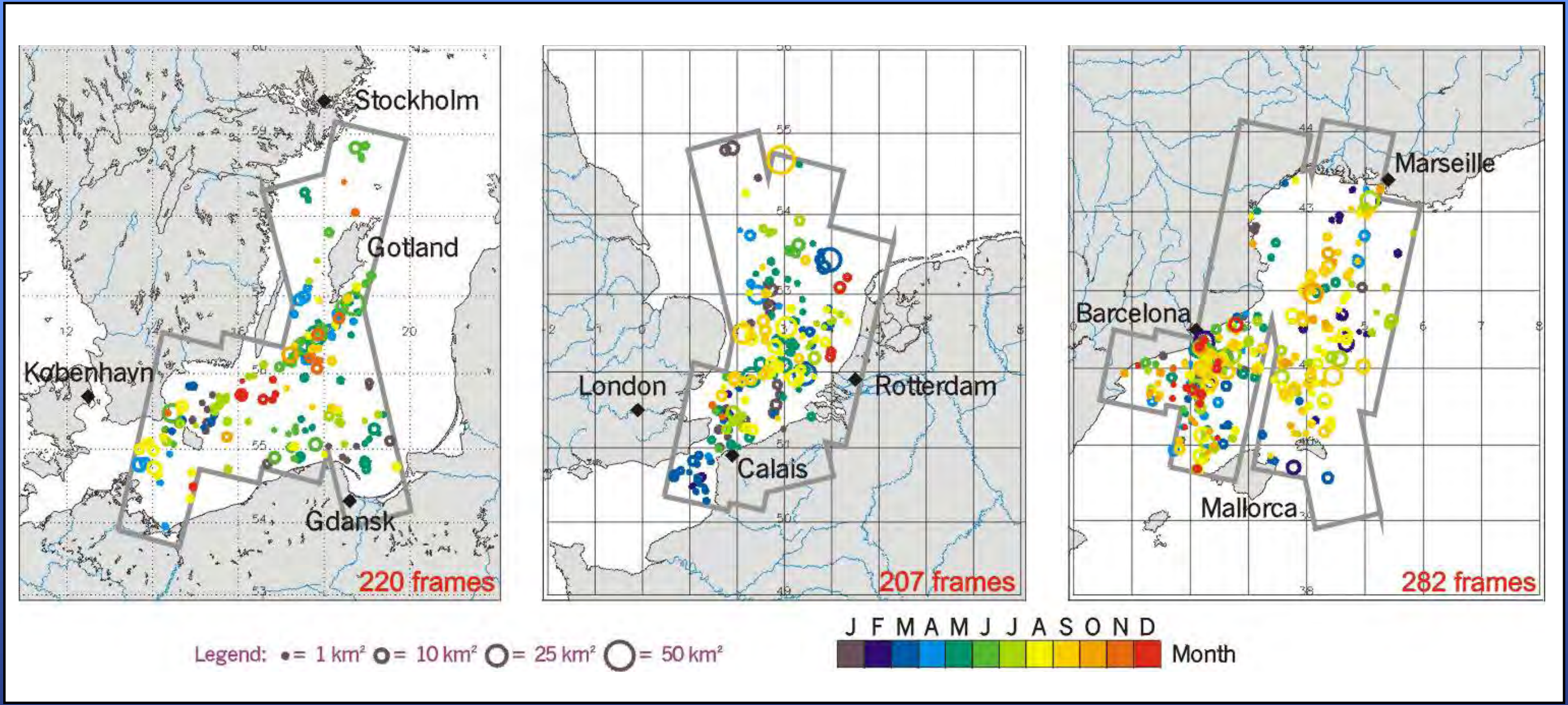

- most pollution along main ship traffic routes
- more pollution during summer ?

Statistical Analysis of SAR Images

Wind Speed Dependency of Radar Contrast

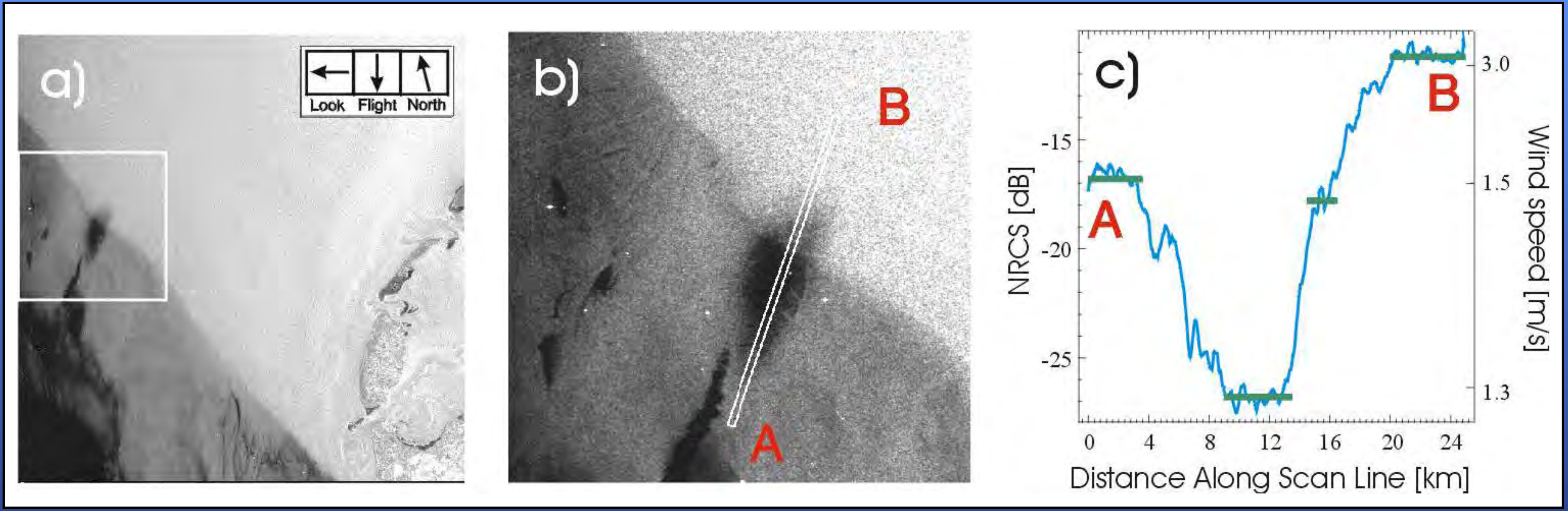

ERS-2 SAR image; 24 March 1997 / 1040 UTC

(orbit 10068, frame 2529)

Statistical Analysis of SAR Images

Normalized Visibility

Defined as ratio A/B of the wind speed distribution of detected oil spills (A) and model winds (B)

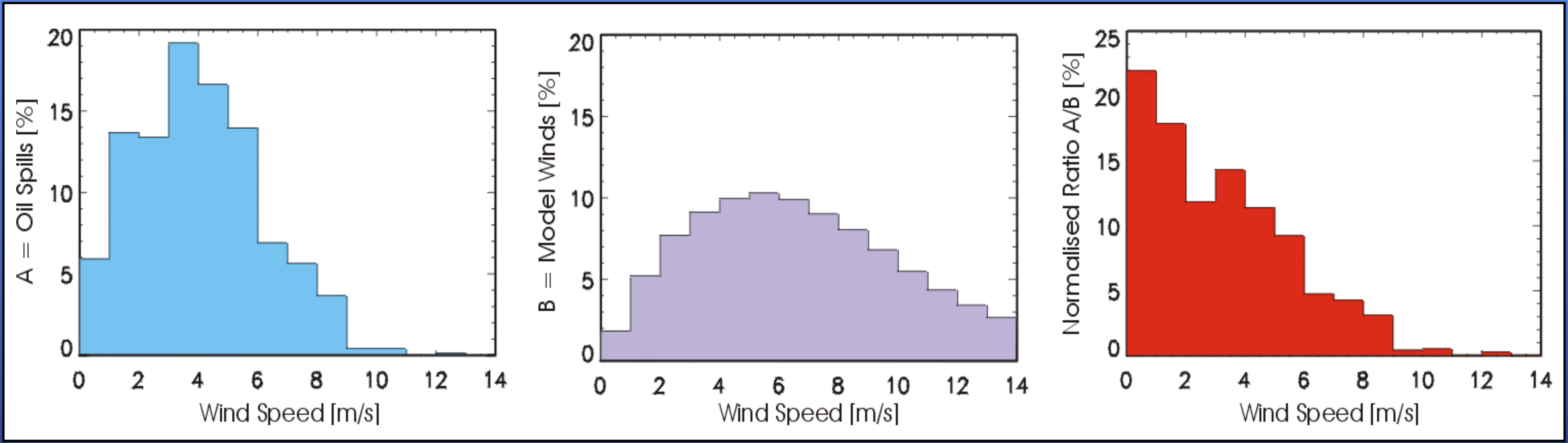

Any oil pollution in the three CS test sites is visible only at wind speeds up to 9-10 m/s !

Statistical Analysis of SAR Images

Only those oil spills considered which were detected at low to moderate winds (U < 9m/s)

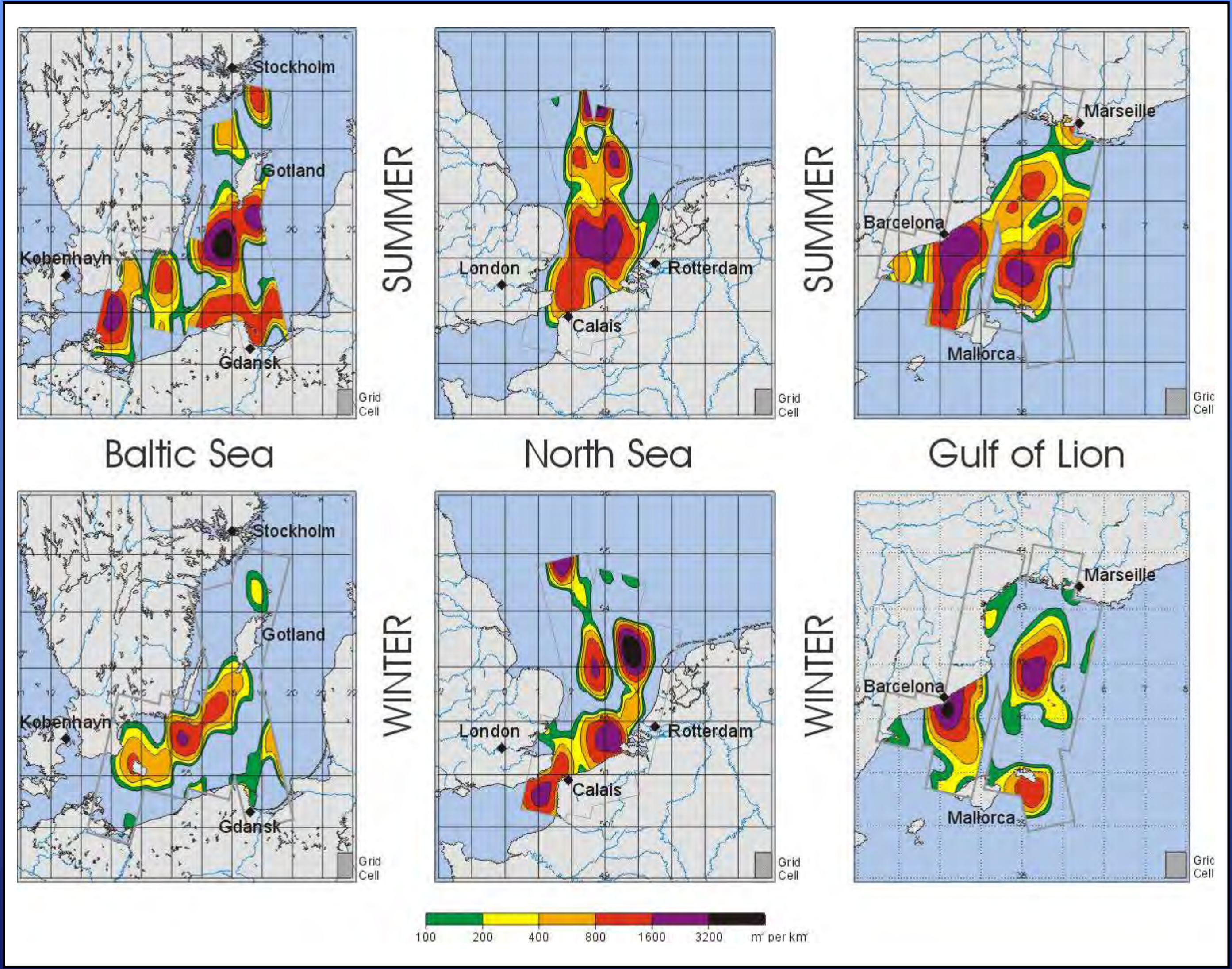

Statistical Analysis of SAR Images

Fractal Dimension

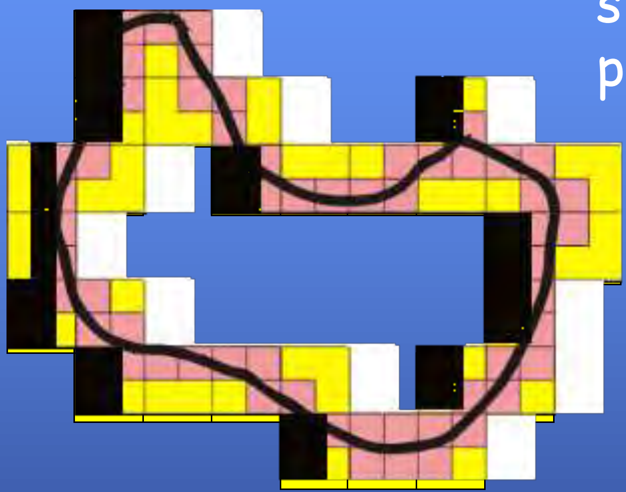

Box counting algorithm to detect self-similar characteristics of different phenomena:

$$D = -\log[N_e] / \log[e]$$

Calculate box counting dimensions for different image intensity levels i (NRCS):

$$D(i) = -\log[N_e(i)] / \log[e]$$

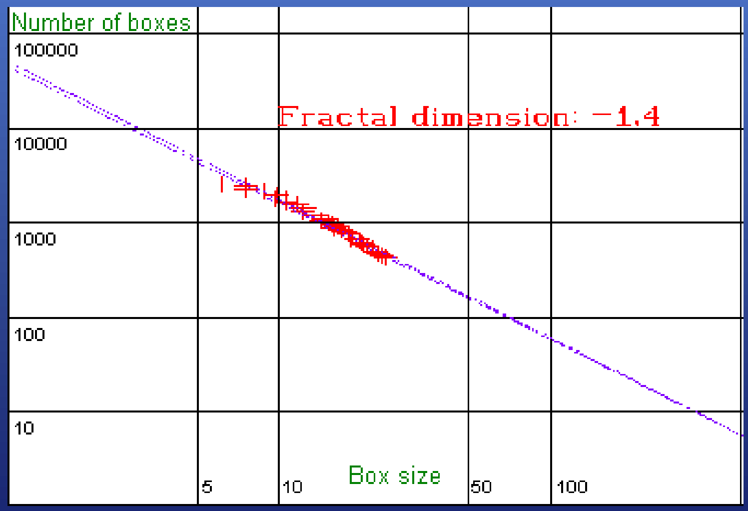

Statistical Analysis of SAR Images
Fractal Dimensions

Examples of functions *D(i)* for different oceanic and atmospheric phenomena

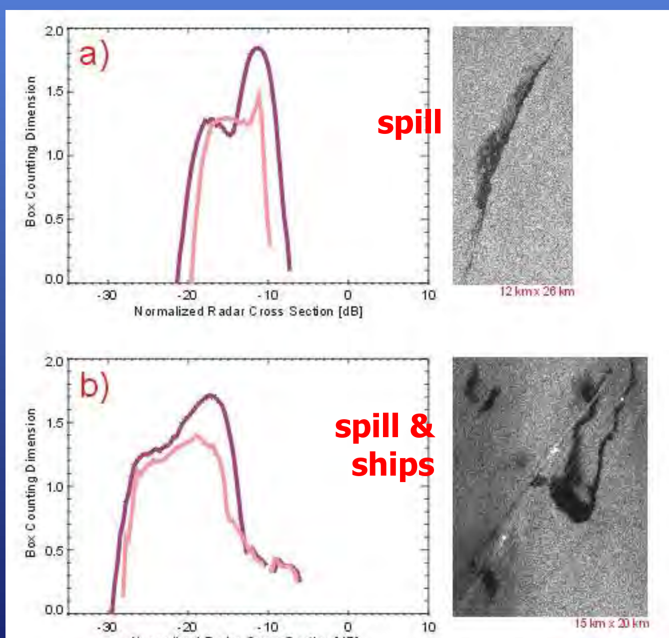

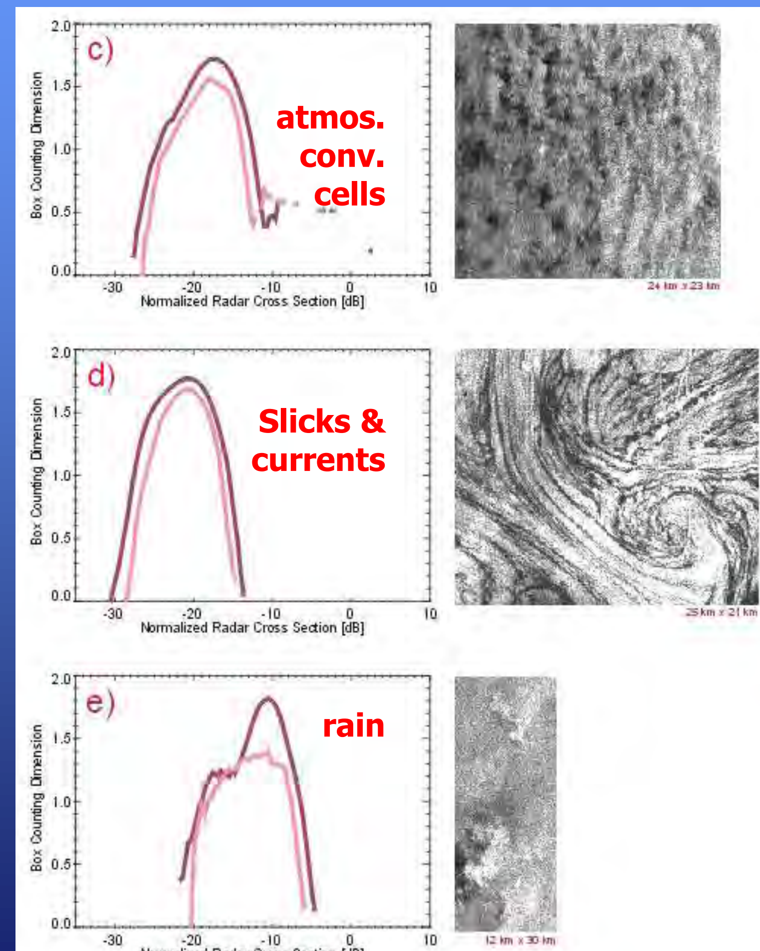

purple:
no filter

pink:
Kuan filter

Rain

Rain Cells on SAR Images

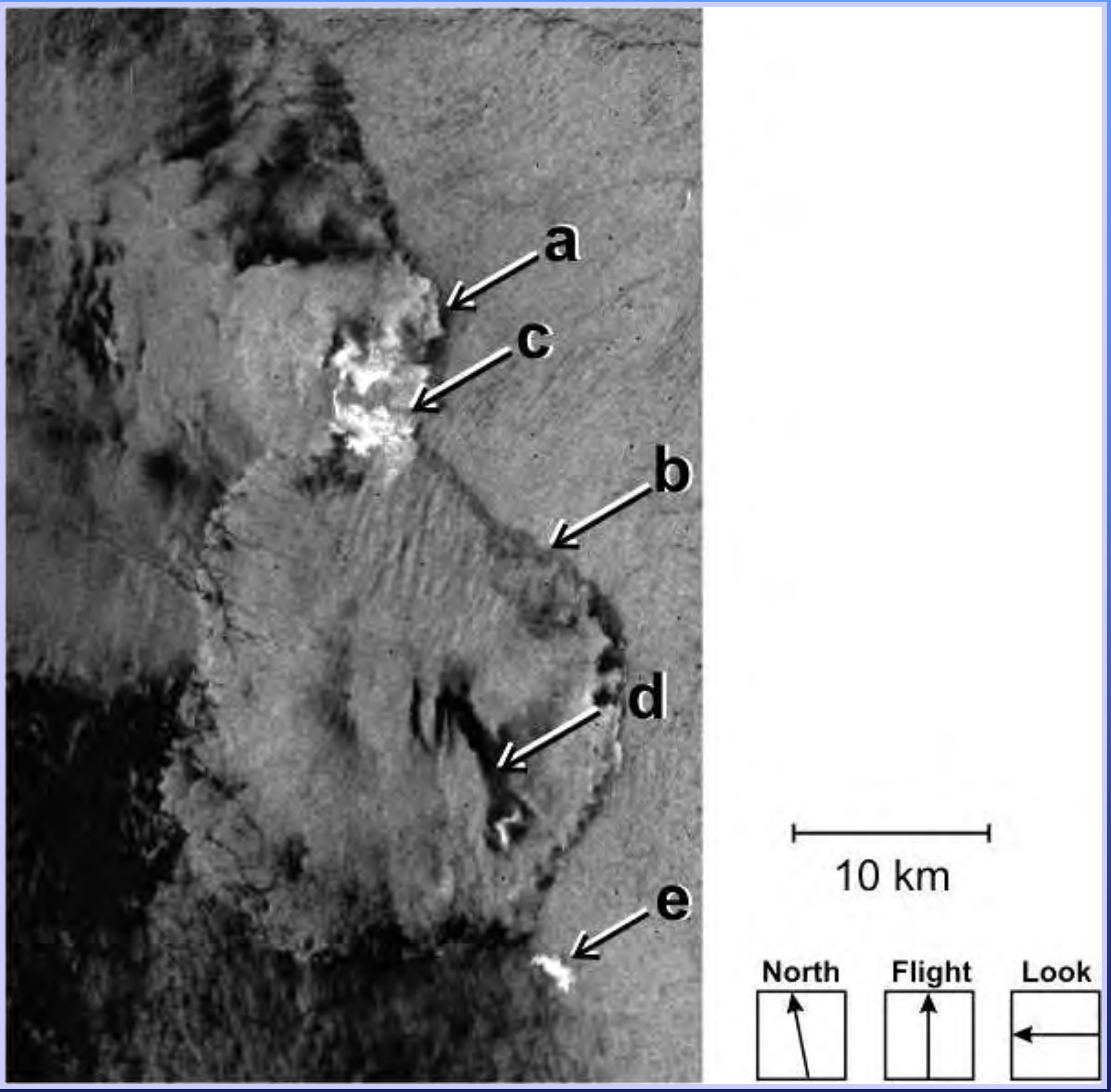

ERS-2

South China Sea

May 11, 1998,
0246 UTC

Universität Hamburg

Rain Cells on SAR Images

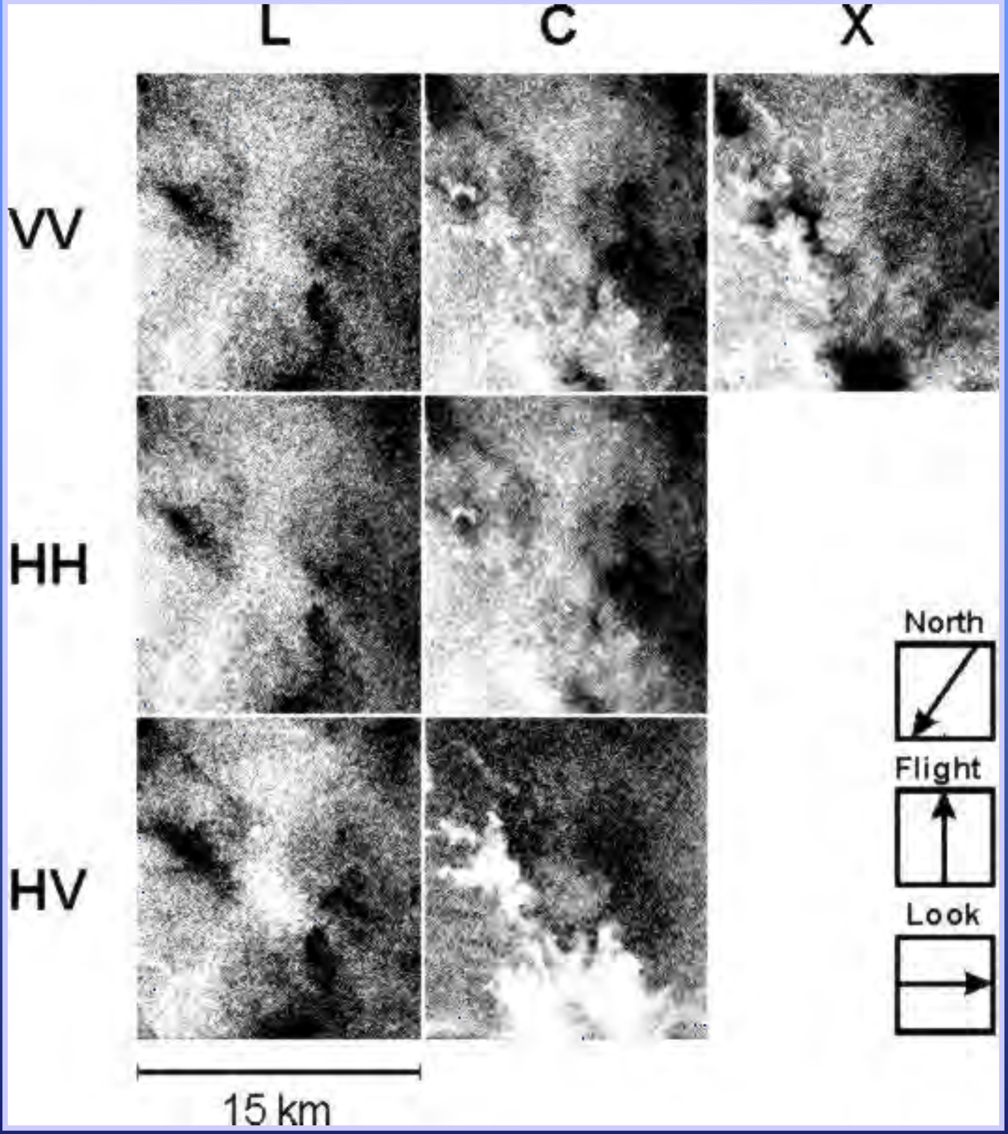

SIR-C/X-SAR

Carribean Sea

April 17, 1994,
17:56 UTC

Rain Cells on SAR Images

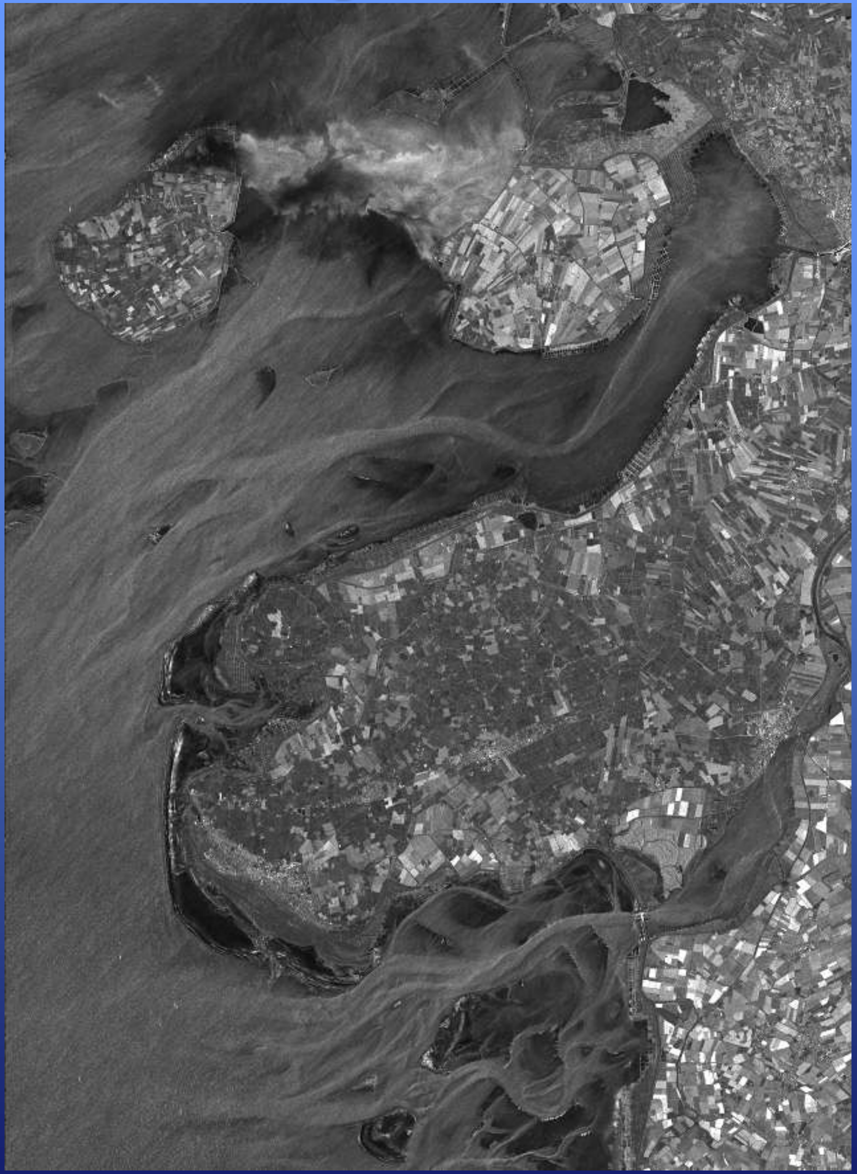

TerraSAR-X

German Bight
21 August 2008,
05:50 UTC

Field Experiments / North Sea

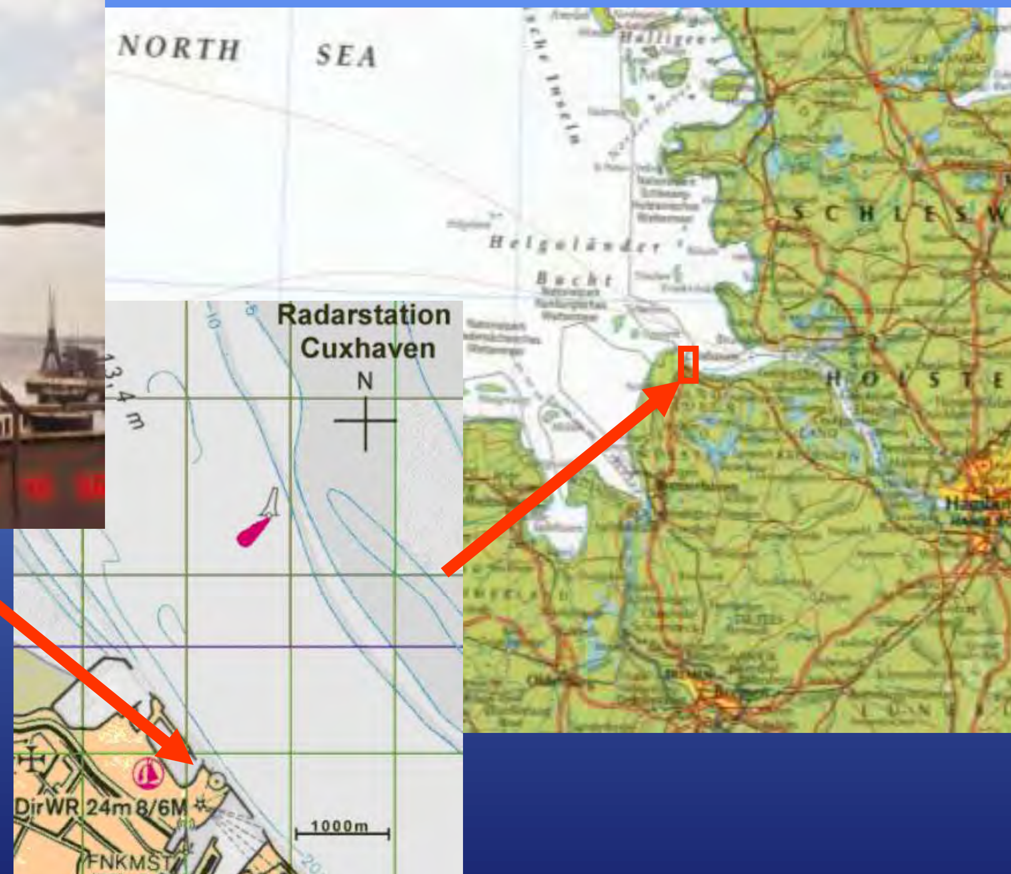

L, S, C, X band (1-10 GHz)
HH-, VV-, HV-polarization
θ = 35...70°
h = 24m
R = 0…50 mm/h

Field Experiments : Results

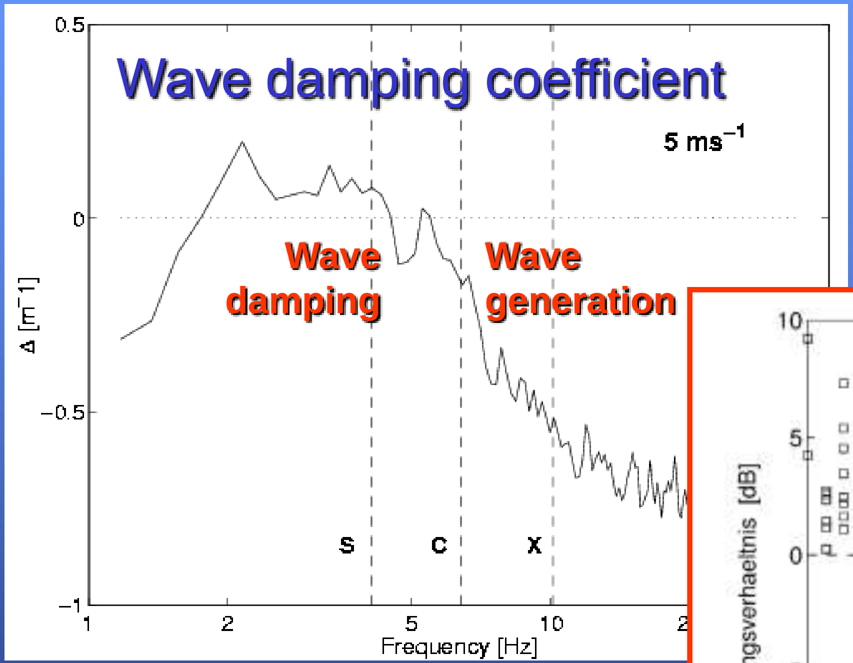

Rain rates up to 50 mm/h

S band: RCS reduction,
C band: same values
X band: RCS enhancement

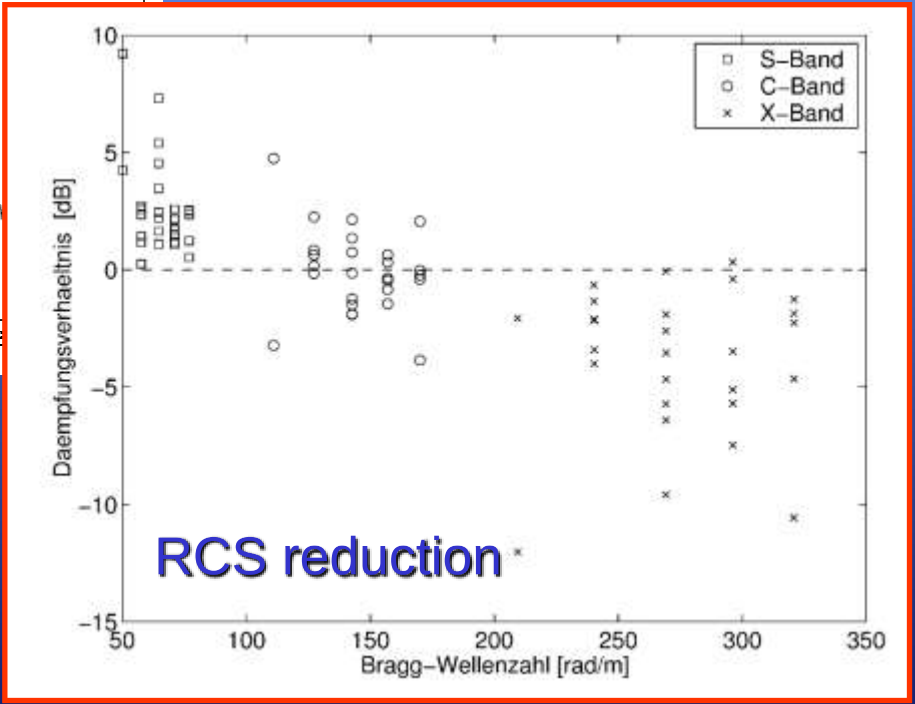

Braun, 2002

Multi^3 Scat on FINO 2

Direct Link Between σ_0 and k

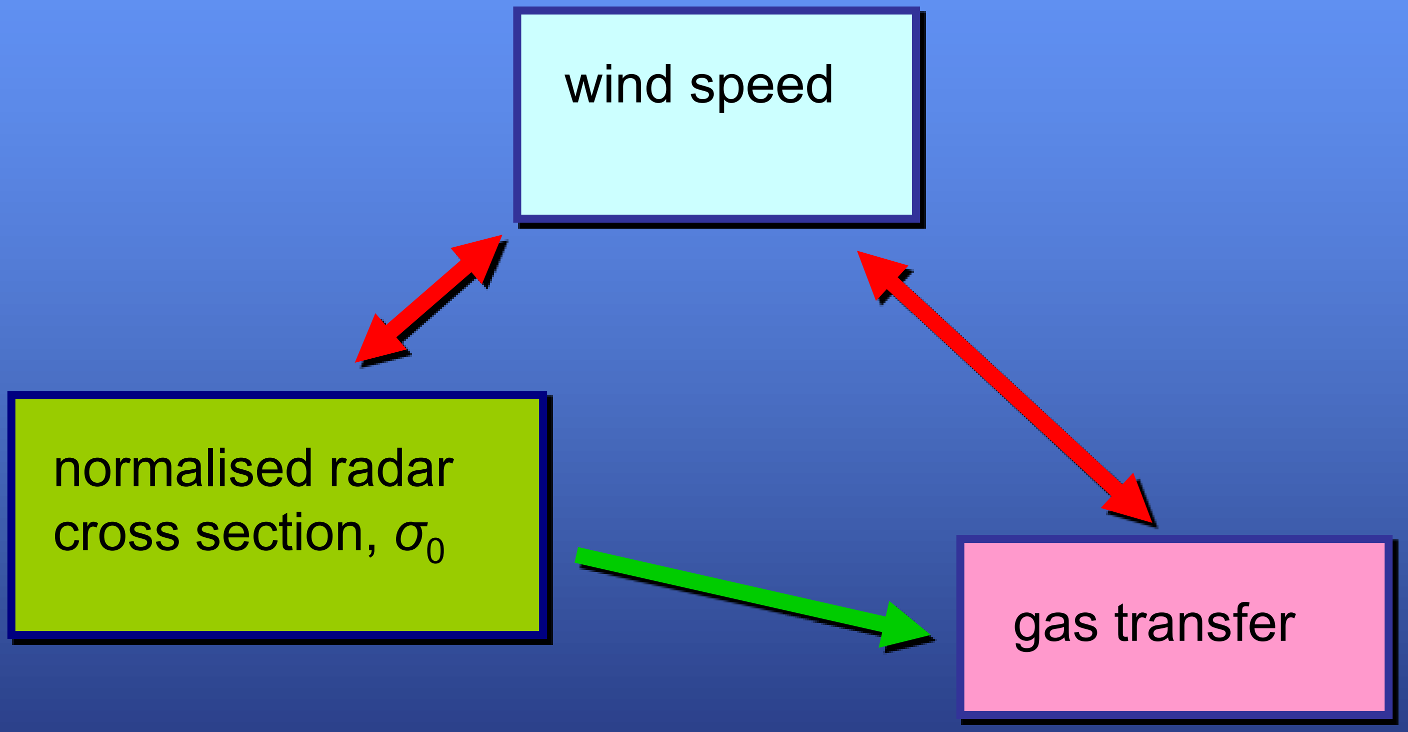

Multi³ Scat:

- 5 radar frequencies (L,S,C,X,Ku) 1..15 GHz
  - (cf. cellphone 0.9 GHz (D) – 1.8 GHz (E))
- 4 polarizations (HH,HV,VV,VH)
- Transmit power < 1 W total
  - (cf. cellphone 1 W - 2 W)
- Incidence angle 31°..65°

Radar backscatter as measure of the sea surface roughness

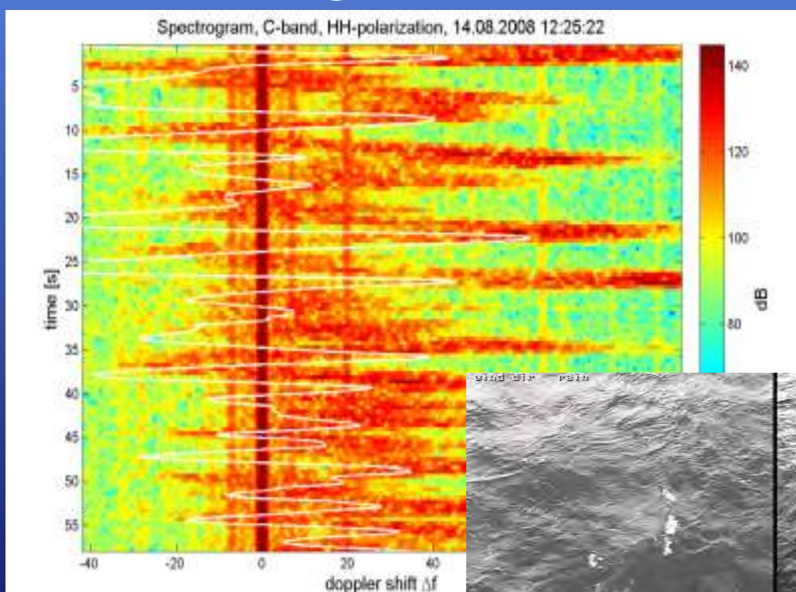

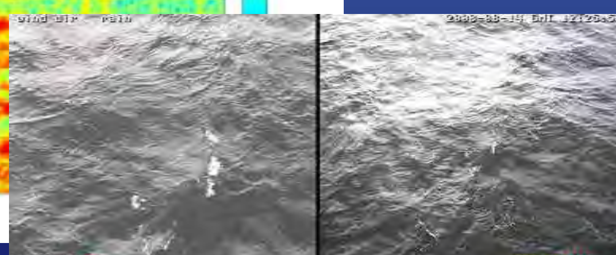

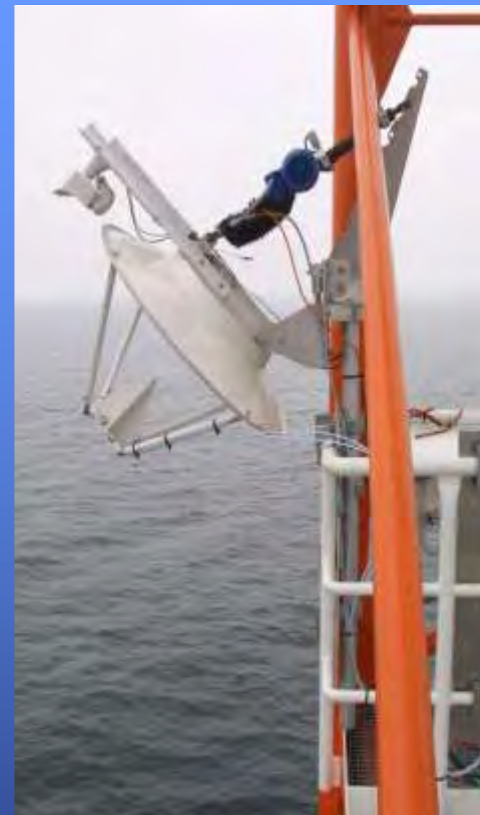

Multi ³ Scat @ FINO 2

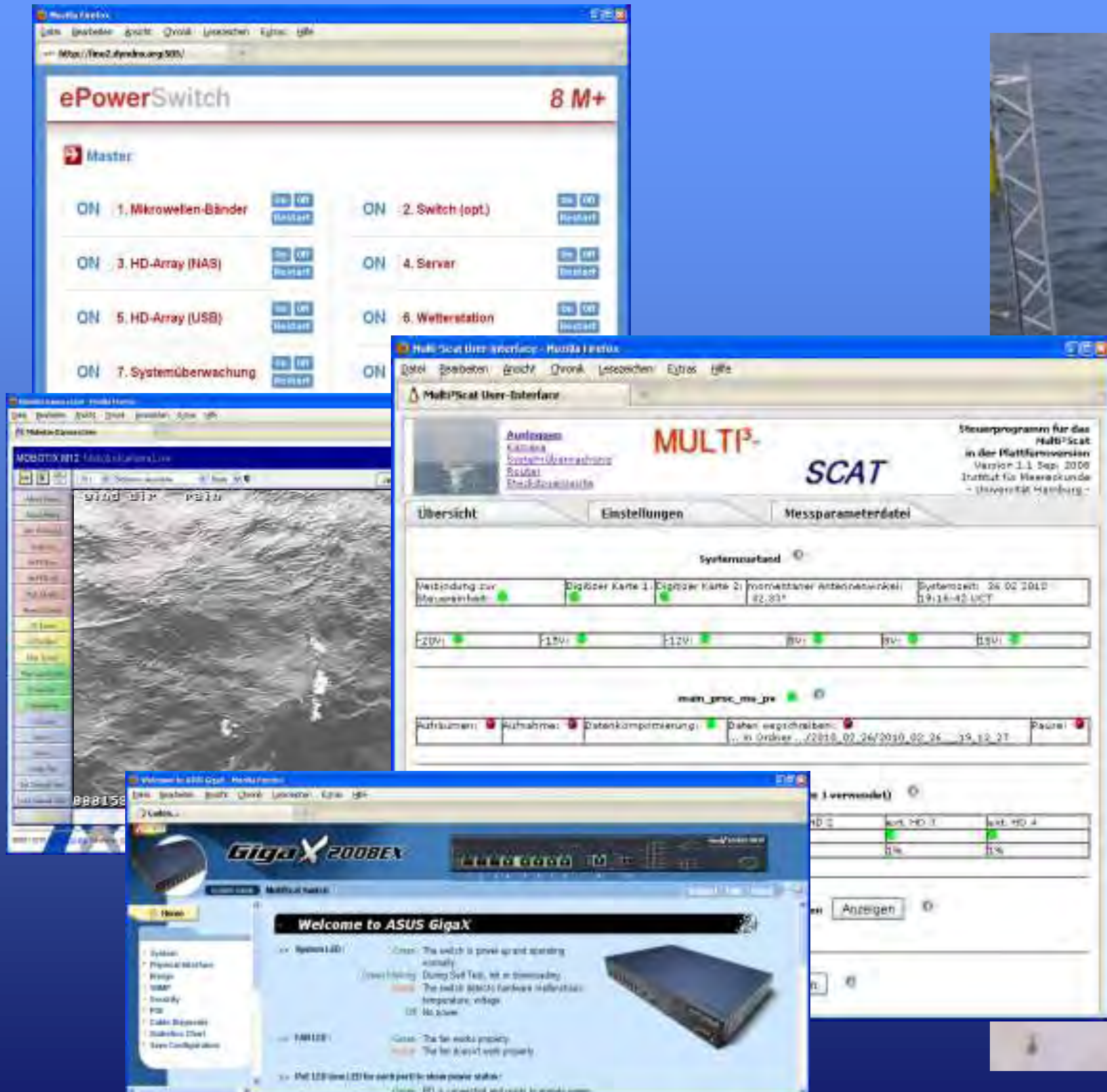

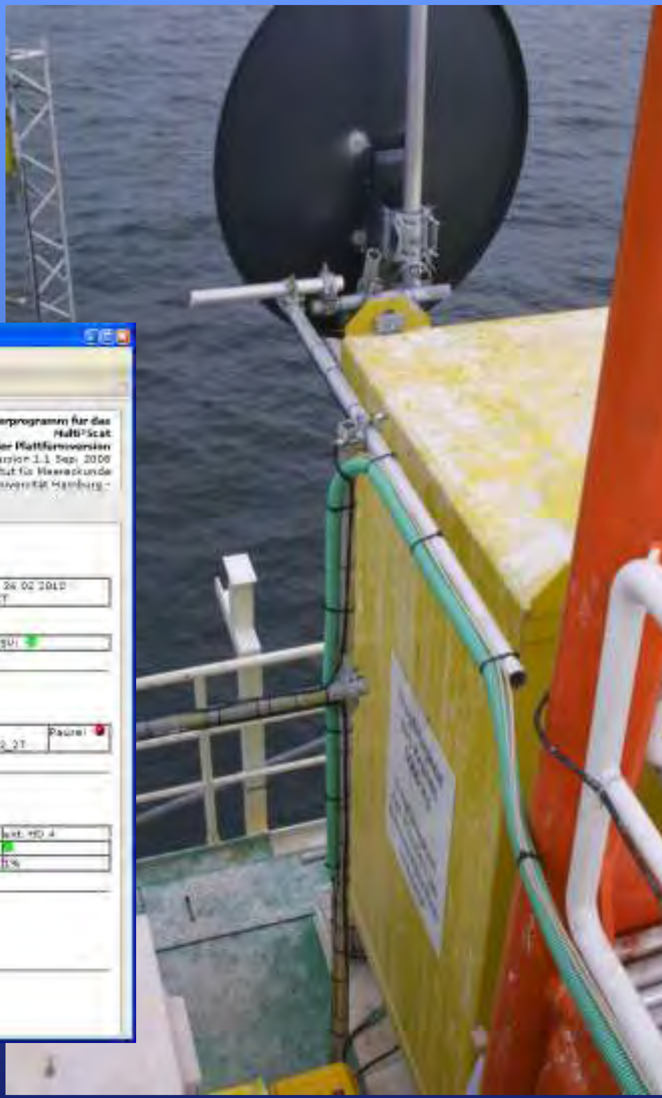

Multi ³ Scat @ FINO 2

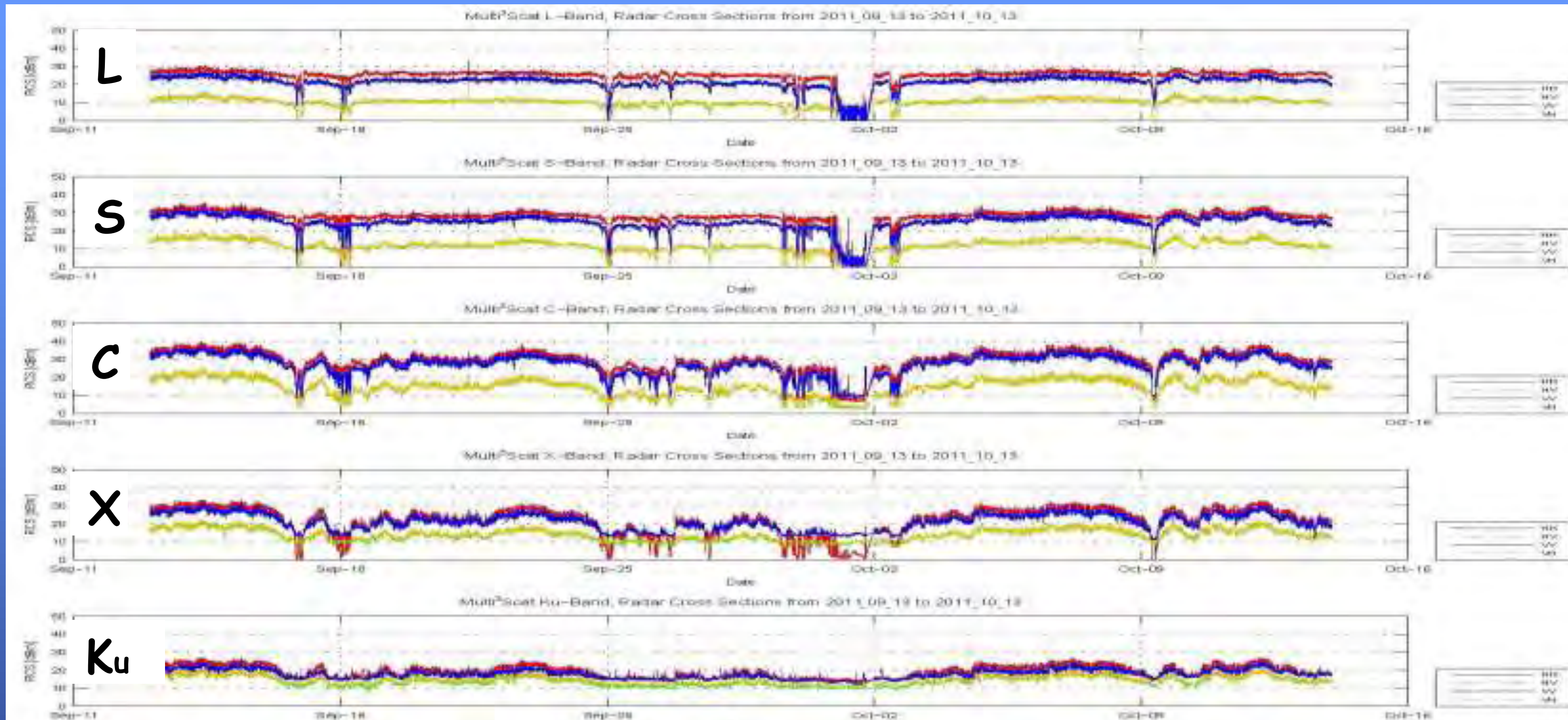

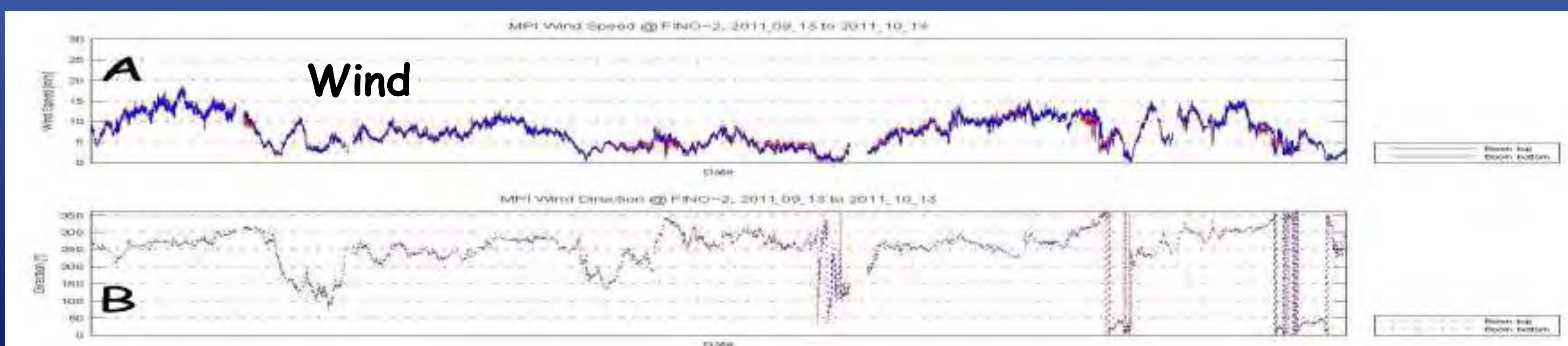

wind-driven processes in the Mediterranean Sea

Ligurian-Provençal Sea

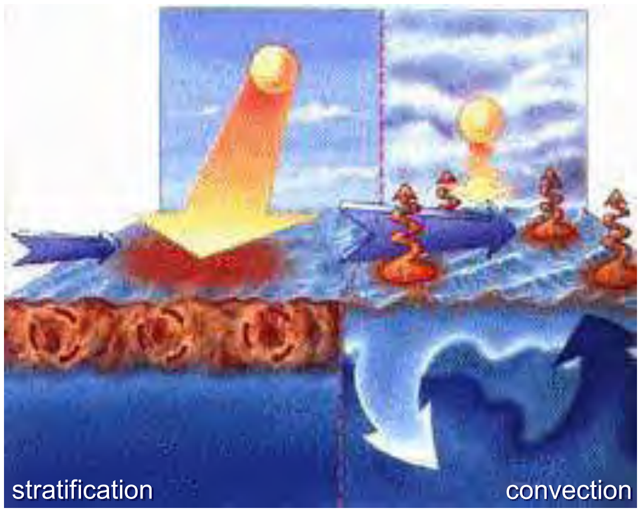

Levantine Basin

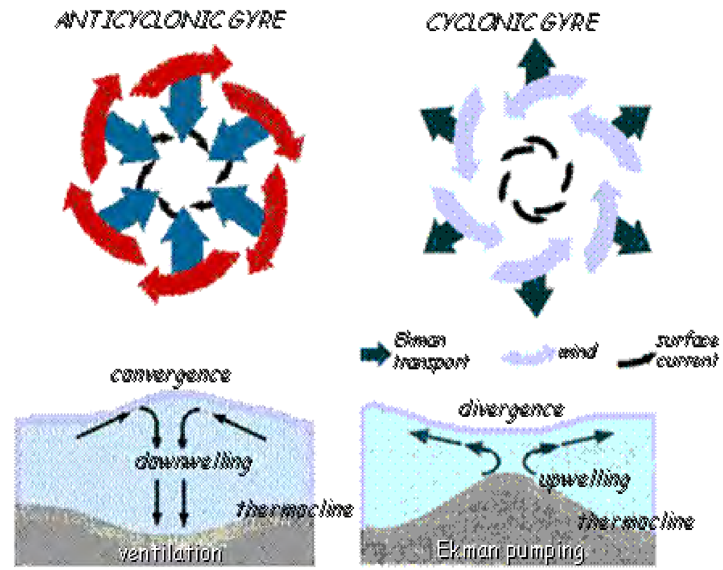

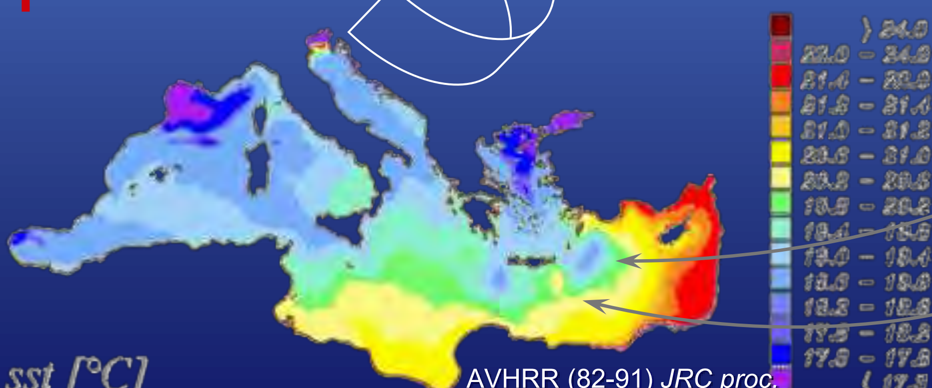

sst [°C]

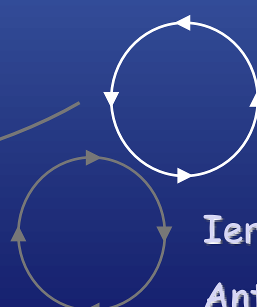

Rhodes Gyre
cyclonic:
upwelling
cold core

Ierapetra Gyre

Anticyclonic: downwelling, warm core

Universität Hamburg

wind-driven blooming patterns in the Mediterranean Sea

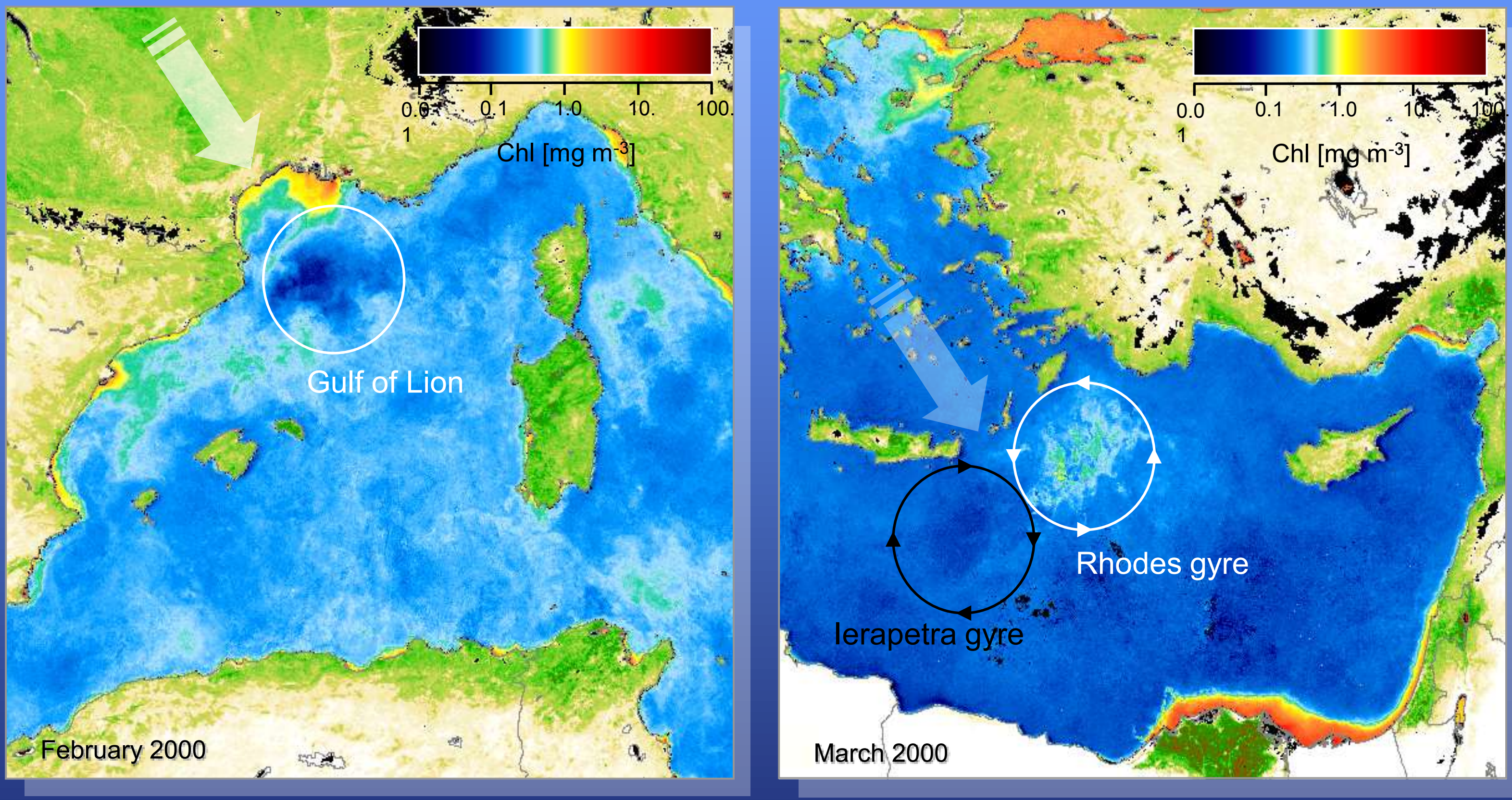

Ligurian-Provençal Sea, monthly mean winds

Wind Speed:

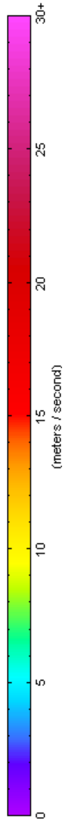

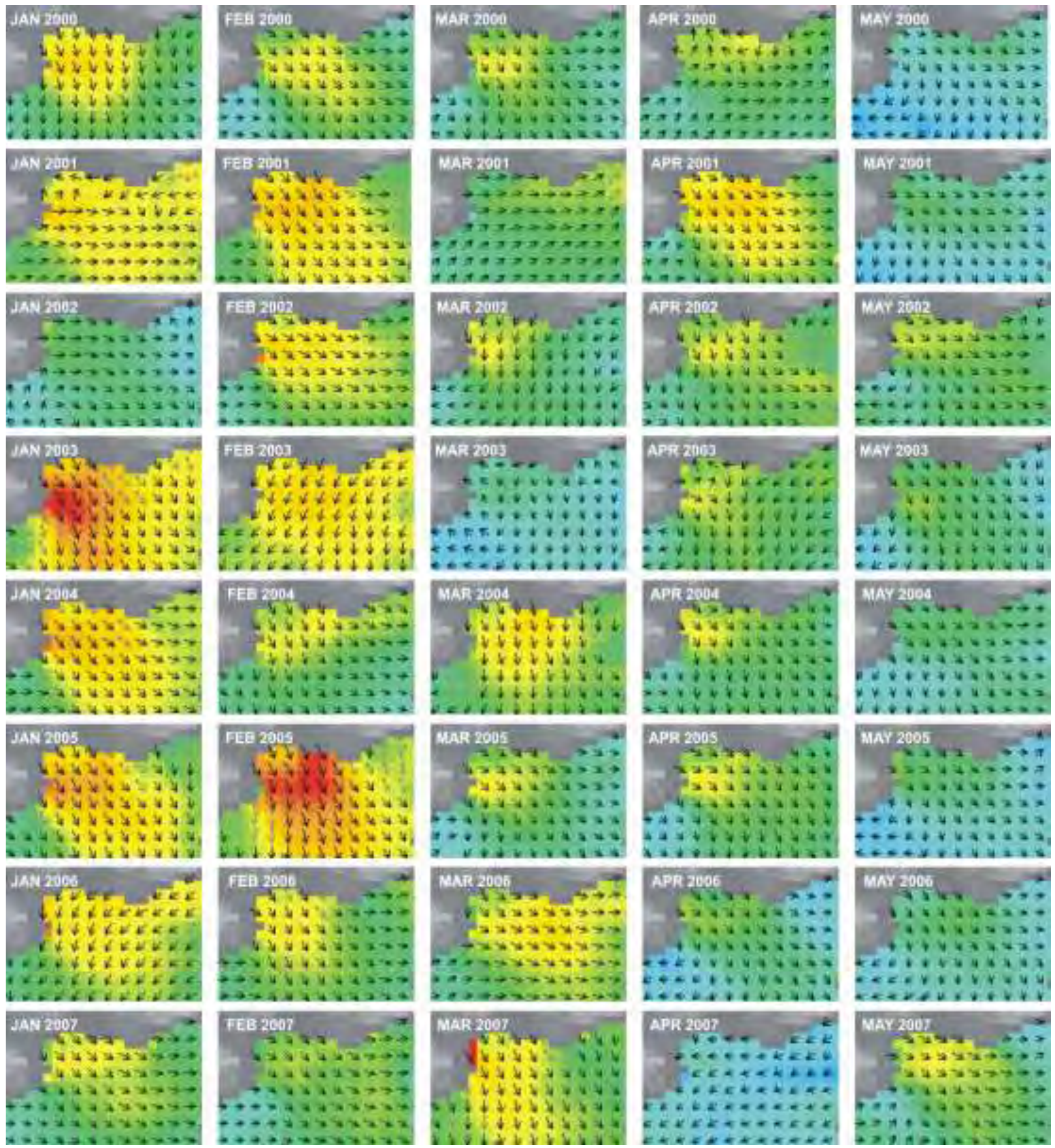

Ligurian-Provençal Sea
monthly mean winds
January to May (columns)
2000 to 2007 (rows)
QuikScat data

Ligurian-Provençal Sea, monthly mean Chl

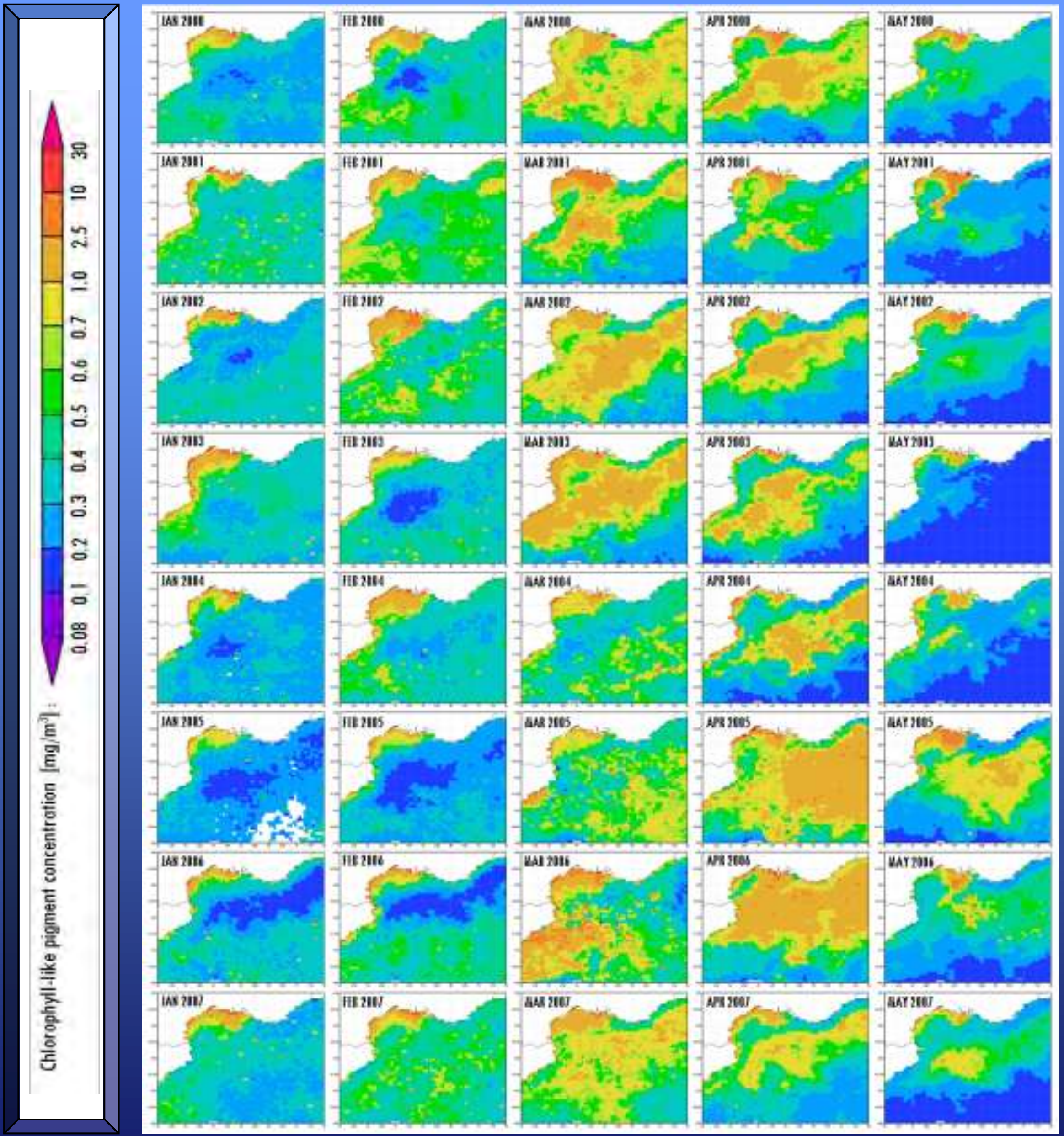

Ligurian-Provençal Sea

monthly mean Chl [mg/m^3]

January through May (columns)

from 2000 to 2007 (rows)

SeaWiFS data, *NASA proc.*

Levantine Basin, monthly mean winds

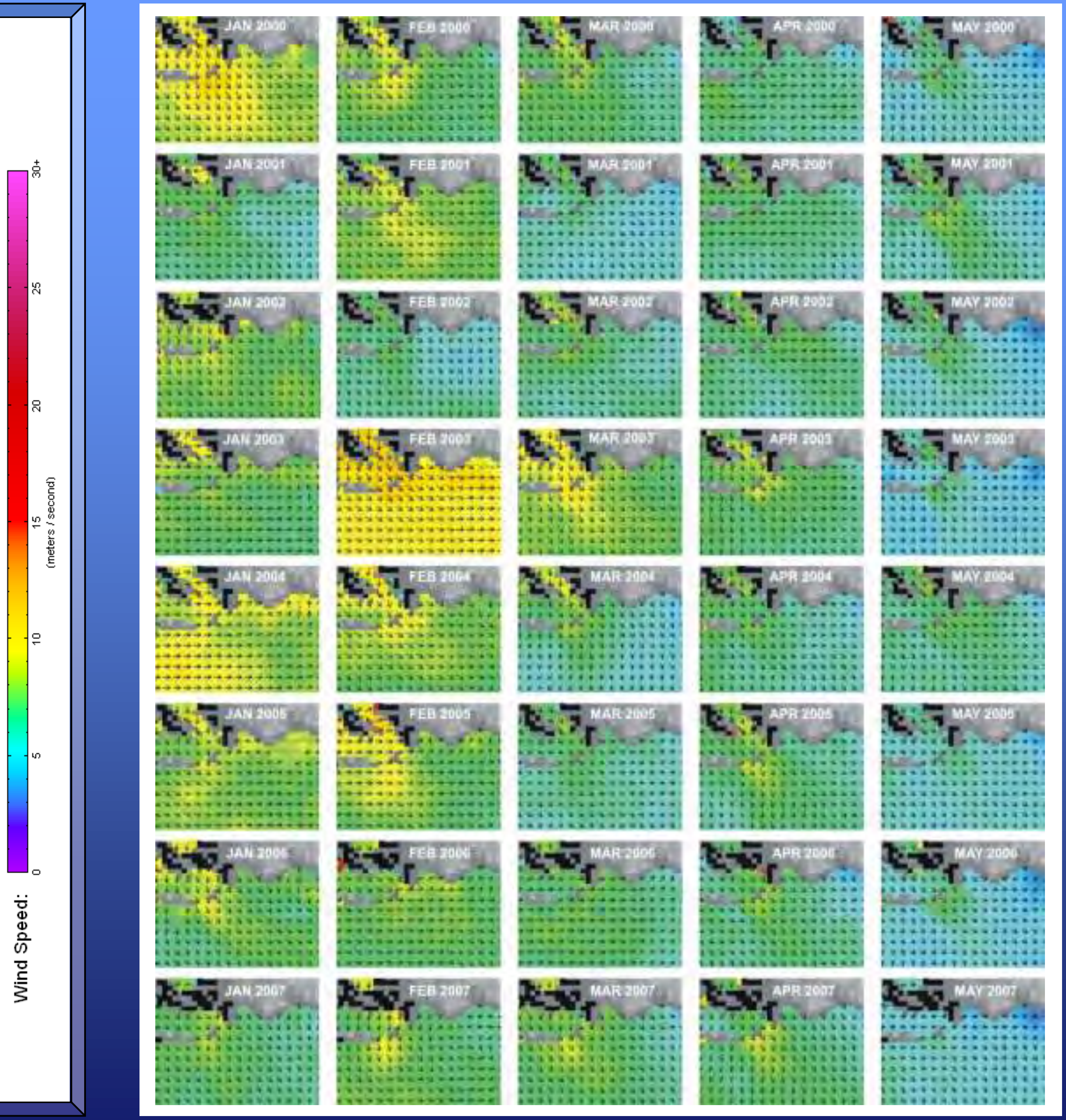

Levantine Basin

monthly mean winds

January to May (columns)

2000 to 2007 (rows)

QuikScat data

Levantine Basin, monthly mean Chl

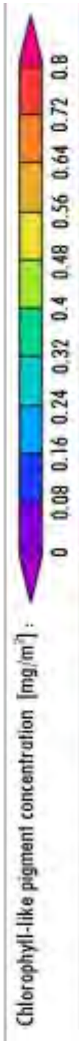

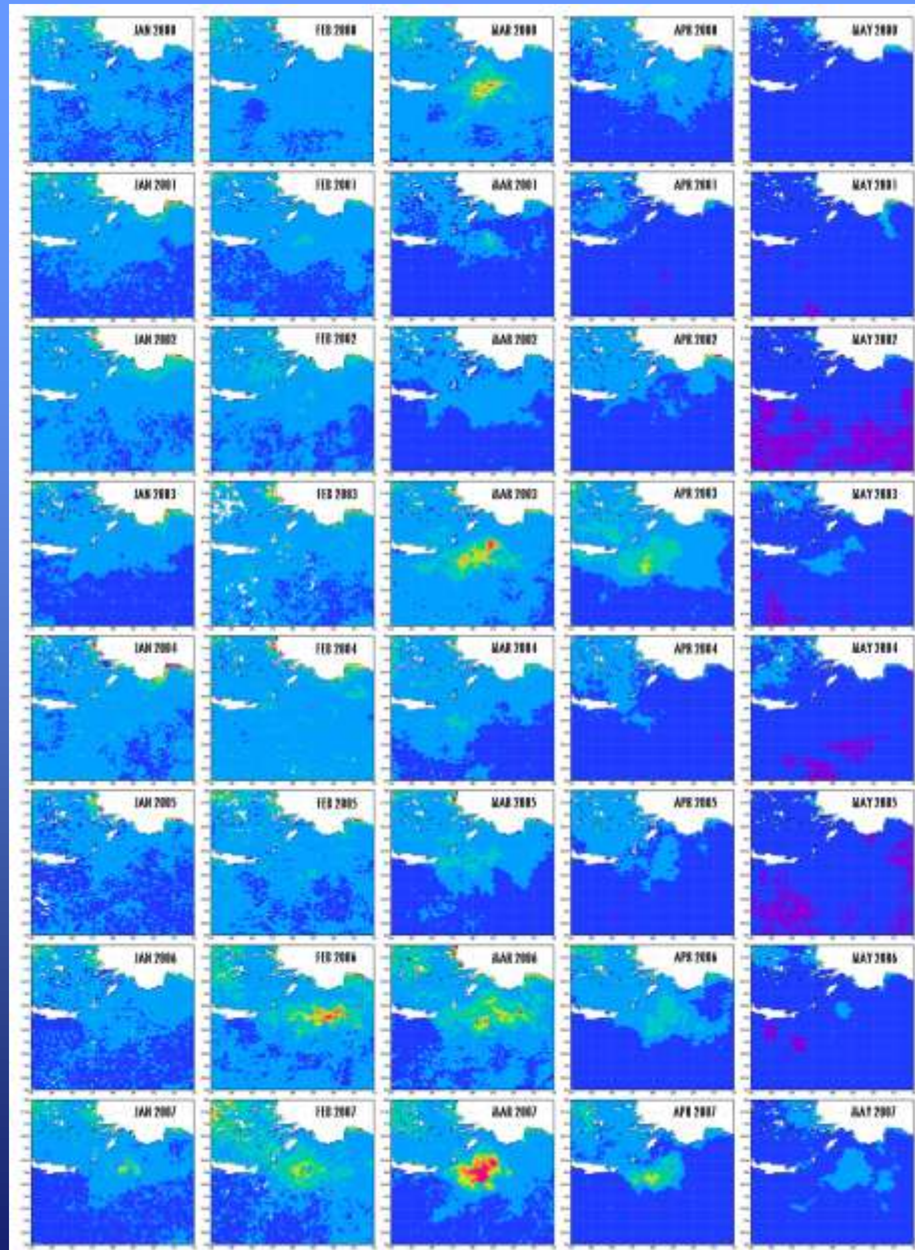

Levantine Basin

monthly mean Chl [mg/m^3]

January through May (columns)

from 2000 to 2007 (rows)

SeaWiFS data, *NASA proc.*

Summary

SAR signatures of marine surface films, bottom topography, rain and sea ice

UHH's Multi³Scat: multi-frequency scatterometer to be operated from helicopters or platforms

Field experiments in the German Bight with (quasi-) biogenic and anthropogenic surface films: investigations on the use of radar for the discrimination of surface film types

Discrimination possible at low to moderate winds, impossible at high winds

Continuous scat measurements on platform FINO2 in the western Baltic Sea

Joint use of Scat and OC Data in the Med Sea

Благодарю за внимание !

"It may be wrong, but it's how I feel."

Благодарю за внимание !